Probabilistic Engineering Mechanics 68 (2022) 103230

Contents lists available at ScienceDirect

Probabilistic Engineering Mechanics

journal homepage: www.elsevier.com/locate/probengmech

Continuous random field representation of stochastic moving loads

Thomas Golecki [a,*], Fernando Gomez [b], Juan Carrion [c,d], Billie F. Spencer Jr. [a]

[a] Civil and Environmental Engineering, University of Illinois at Urbana–Champaign, 205 N Mathews Ave, Urbana, 61801, IL, USA
[b] College of Science and Engineering, Universidad San Francisco de Quito, Diego de Robles y Via Interoceanica, Quito, Ecuador
[c] Skidmore, Owings & Merrill, LLP, 224 S Michigan Ave #1000, Chicago IL, 60604, IL, USA
[d] Department of Civil Engineering, University of Cuenca, Cuenca, Ecuador

ARTICLE INFO

Keywords:
Moving loads
Stochastic dynamics
Lyapunov equation
Padé approximation

ABSTRACT

While the problem of random loads moving across a beam has been studied extensively, the existing methods are limited in terms of their applicability. The most common approach uses modal superposition, which requires that the load be represented in terms of the structure's mode shapes, making the representation of the load intrinsically a function of the structure to which it is applied. To address this problem, this paper approximates the discrete stochastic moving load as a white noise passed through filters constructed with Padé approximants. The resulting model of the load is independent of the structure and enables efficient random vibration methods to be applied for solution of the problem. By representing the structure and the loading together in an augmented state space system, the variance of responses can be found directly and accurately, enabling the traffic-induced responses of a broader class of bridge structures to be analyzed. The effectiveness and usefulness of the proposed approach is demonstrated through two examples of bridge structures.

1. Introduction

Bridges are critical components of transportation networks and ensuring their continued safe and reliable operation is imperative. An important part of this process is understanding their response to traffic loading. The AASHTO LRFD bridge design procedures use static analysis of heavy trucks, amplified by calibrated impact and loading factors, compared to a factored resistance to estimate a bridge's structural reliability [1]. Even when site-specific vehicle loading statistics acquired via weigh-in-motion technology are available, the analysis procedures use a loading factor calibrated for the site-specific loading [2,3]. While the calibrated load factor and static analysis approach is straightforward to implement, it obscures the dynamic nature of the bridge's response to traffic; moreover, the traffic loading is intrinsically random in nature, making the bridge response also random.

Initial efforts toward determining the random traffic-induced response of bridges appeared in the 1960s [4,5] where the traffic was idealized as moving point loads and the bridge as a simple beam. Note that earlier work only considered deterministic moving point loads, a summary of which is provided by Frýba [6]. Also included in [6] is a discussion of other representations of the vehicle loading, a moving mass and a moving oscillator. The assumption of moving force is applicable when ratio of vehicle mass to structural mass is low, as is the case for typical highway bridges. Development of the response of bridges to stochastic moving loads was aided by research in other fields, drawing on the parallels between random traffic loading and shot noise; a compound Poisson processes, comprised of randomly arriving impulses of random magnitude, is applied to a system where the total response is the superposition of responses to individual impulses. For example, Roberts [7] and Lin [8] derived a generalized cumulative response of a linear system to impulses with random magnitude and independent random arrival times. Most of the existing work, follows a similar approach of computing the statistics of the structural responses due to moving loads using modal decomposition, where the loading is represented as functions of the structure's mode shapes [9–11]. The modal approach has been expanded to include different arrival processes and loading pulses [12], as well as to the case of random velocities [13,14] and random load durations using an Erlang renewal process rather than Poisson process [15,16]. Others have also used modal decomposition to compute the power spectral densities (PSD) of the response [14,17]. Because these approaches couple the loading representation to the structure's mode shapes, focus has been limited primarily to idealized simple structures such as simply supported beams; extension to more complex structures is not straightforward.

Alternatively, solutions of the moving load problem that do not couple the loading and the structure are mainly time-domain based, which can be computationally demanding. For example, Mishra et al. [18] used Monte Carlo simulation of stochastic traffic to estimate the PSD of the loading. This approach however is presented only for a specific set of traffic loading parameters. Chen et al. [19] developed a spatio-temporal power spectral density representation of the stochastic

* Corresponding author.
E-mail address: golecki2@illinois.edu (T. Golecki).

https://doi.org/10.1016/j.probengmech.2022.103230
Received 10 November 2021; Received in revised form 1 February 2022; Accepted 2 February 2022
Available online 9 February 2022

moving load. In both approaches, the PSD of the load is multiplied by the squared frequency response function to obtain the PSD of the response and subsequently integrated numerically to obtain the covariances of the structural response. However, these approaches become intractable as the complexity of the structure increases.

Stochastic models of physical phenomena often take the form of a filtered white noise, which for linear systems, allows for direct determination of the response covariances [20]. This approach has been used for efficient optimization of linear structures [21–24] and nonlinear structures [25,26] subjected to stochastic wind and earthquake loads. As for relating the discrete traffic loading to a continuous process, Roberts [7] has shown that in the limit, as the density of arriving impulses increases, the moving load model for traffic loading approaches a white noise. Ditlevsen [27] and Ditlevsen and Madsen [28] approximated the static effects of traffic loading as a translating white noise random field loading; the individual response variance was then computed by integrating the product of the random loading and the spatial influence function over a spatial range. Their work developed a white noise representation of stochastic traffic as a mixture of cars and trucks in terms of various traffic parameters. Additionally, their model is developed for spatial rather than temporal variance. However, the intrinsic dynamic nature of the loading and the associated bridge response was not considered.

This paper proposes a continuous representation of the discrete loading process as the sum of a static mean load and a filtered white noise stochastic load that is computationally efficient and is not dependent of the structure to which it is applied. This continuous spatio-temporal random field characterization of the stochastic moving loads is discretized in space, yielding a filtered vector white noise process, whose state space realization is obtained using Padé approximants. Combining this model of the loading process with the state space model of the structure yields an augmented representation of the structure-loading system, for which the input is a stationary white noise excitation. Subsequently, the response variances are computed via solution of the Lyapunov equation [20]. Examples for two bridge structures are provided and compared to traditional methods. The results demonstrate the efficacy of the proposed approach to analyze a broad class of bridge structures subjected to stochastic traffic loads.

2. Brief review of random vibration theory

This section presents a brief review of the method used to determine the stochastic response of linear systems subjected to a filtered white noise input. Motivation for representing the moving load as a filtered white noise is also provided.

2.1. System representation

The equation of motion (EOM) of a bridge structure can be represented as

$$\mathbf{M}\ddot{\mathbf{u}} + \mathbf{C}\dot{\mathbf{u}} + \mathbf{K}\mathbf{u} = \mathbf{G}\mathbf{f}\,(t) \tag{1}$$

where $\mathbf{u}$ is the vector of structural displacements, $\mathbf{M}, \mathbf{C}$, and $\mathbf{K}$ are the structure's mass, damping and stiffness matrices, respectively, and $\mathbf{G}$ is the load effects matrix, which maps the input vector $\mathbf{f}\,(t)$ to specific degrees-of-freedom of the structural model. Here, $\mathbf{f}\,(t)$ represents the stochastic moving load process, which has been spatially discretized.

This system can be represented in state space form as

$$\begin{aligned}\dot{\mathbf{x}}_\mathrm{s} &= \mathbf{A}_\mathrm{s}\mathbf{x}_\mathrm{s} + \mathbf{B}_\mathrm{s}\mathbf{f}\,(t)\\ \mathbf{y} &= \mathbf{C}_\mathrm{s}\mathbf{x}_\mathrm{s} + \mathbf{D}_\mathrm{s}\mathbf{f}\,(t)\end{aligned} \tag{2}$$

where $\mathbf{x}_\mathrm{s} = \begin{bmatrix}\mathbf{u}\\ \dot{\mathbf{u}}\end{bmatrix}$, and the system matrices $\mathbf{A}_\mathbf{s}$ and $\mathbf{B}_\mathbf{s}$ are defined as

$$\mathbf{A}_\mathbf{s} = \begin{bmatrix}\mathbf{0} & \mathbf{I}\\ -\mathbf{M}^{-1}\mathbf{K} & -\mathbf{M}^{-1}\mathbf{C}\end{bmatrix}, \quad \mathbf{B}_\mathbf{s} = \begin{bmatrix}\mathbf{0}\\ \mathbf{M}^{-1}\mathbf{G}\end{bmatrix} \tag{3}$$

The output matrices $\mathbf{C}_\mathbf{s}$ and $\mathbf{D}_\mathbf{s}$ are defined as needed for the output responses of interest. In $\mathbf{A}_\mathbf{s}$, $\mathbf{0}$ is a square matrix of zeros and $\mathbf{I}$ is identity matrix with sizes corresponding to the number of degrees-of-freedom (dof) in the model. In $\mathbf{B}_\mathbf{s}$, $\mathbf{0}$ is a matrix of zeros with a row for each model dof and a column for each input.

Many stochastic excitations can be represented as a linear system whose input is a filtered white noise process [20] given by

$$\begin{aligned}\dot{\mathbf{x}}_\mathrm{f} &= \mathbf{A}_\mathrm{f}\mathbf{x}_\mathrm{f} + \mathbf{B}_\mathrm{f}\mathbf{w}\,(t)\\ \mathbf{f} &= \mathbf{C}_\mathrm{f}\mathbf{x}_\mathrm{f}\end{aligned} \tag{4}$$

where $\mathbf{w}\,(t)$ is a vector white noise input process in which

$$\begin{aligned}\mathbb{E}\left[\mathbf{w}\,(t)\right] &= 0\\ \mathbb{E}\left[\mathbf{w}\,(t)\,\mathbf{w}\,(t-\tau)\right] &= 2\pi\mathbf{S}_0\delta\,(\tau)\end{aligned} \tag{5}$$

where $\mathbb{E}\left[\cdot\right]$ is the expected value operator. The matrices $\mathbf{A}_\mathrm{f}$, $\mathbf{B}_\mathrm{f}$ and $\mathbf{C}_\mathrm{f}$ define the loading filter system, $\mathbf{x}_\mathrm{f}$ represents the states of this system, and $\mathbf{f}\,(t)$ is the output vector function, and $\mathbf{S}_0$ is the constant two-sided power spectral density matrix for the vector white noise. The details on how to obtain the excitation representation given in Eq. (4) for the stochastic traffic loading are presented in Section 4.

Then, the structural and loading systems can be combined into a single augmented system as

$$\begin{aligned}\dot{\mathbf{x}}_\mathrm{a} &= \mathbf{A}_\mathrm{a}\mathbf{x}_\mathrm{a} + \mathbf{B}_\mathrm{a}\mathbf{w}\,(t)\\ \mathbf{y} &= \mathbf{C}_\mathrm{a}\mathbf{x}_\mathrm{a}\end{aligned} \tag{6}$$

where the augmented state vector is

$$\mathbf{x}_\mathrm{a} = \begin{bmatrix}\mathbf{x}_\mathrm{s}\\ \mathbf{x}_\mathrm{f}\end{bmatrix} \tag{7}$$

and the augmented system matrices $\mathbf{A}_\mathrm{a}$, $\mathbf{B}_\mathrm{a}$ and $\mathbf{C}_\mathrm{a}$ are defined as

$$\begin{aligned}\mathbf{A}_\mathrm{a} &= \begin{bmatrix}\mathbf{A}_\mathrm{s} & \mathbf{B}_\mathrm{s}\mathbf{C}_\mathrm{f}\\ \mathbf{0} & \mathbf{A}_\mathrm{f}\end{bmatrix} \quad \mathbf{B}_\mathrm{a} = \begin{bmatrix}\mathbf{B}_\mathrm{s}\mathbf{D}_\mathrm{f}\\ \mathbf{B}_\mathrm{f}\end{bmatrix}\\ \mathbf{C}_\mathrm{a} &= \begin{bmatrix}\mathbf{C}_\mathrm{s} & \mathbf{D}_\mathrm{s}\mathbf{C}_\mathrm{f}\end{bmatrix}\end{aligned} \tag{8}$$

where $\mathbf{0}$ is a matrix of zeros with a row for each state in the loading system and a column for each state in the structural system.

2.2. Stochastic structural response

The covariance matrix for the states of the augmented system is governed by the Lyapunov differential equation [20].

$$\dot{\mathbf{\Gamma}}_\mathrm{x} = \mathbf{A}_\mathrm{a}\mathbf{\Gamma}_\mathrm{x} + \mathbf{\Gamma}_\mathrm{x}\mathbf{A}_\mathrm{a}^\mathrm{T} + 2\mathbf{B}_\mathrm{a}\mathbf{S}_0\mathbf{B}_\mathrm{a}^\mathrm{T} \tag{9}$$

where covariance matrix is given by

$$\mathbf{\Gamma}_\mathrm{x} = \mathbb{E}\left[\left(\mathbf{x}_\mathrm{a} - \boldsymbol{\mu}_{\mathbf{x}_\mathrm{a}}\right)\left(\mathbf{x}_\mathrm{a} - \boldsymbol{\mu}_{\mathbf{x}_\mathrm{a}}\right)^\mathrm{T}\right] \tag{10}$$

where $\mathbf{x}_\mathrm{a}$ is the response of interest and $\boldsymbol{\mu}_{\mathbf{x}_\mathrm{a}}$ is the mean value of that response. For a linear time invariant system, as time goes to infinity, the system reaches stationarity, i.e., $\dot{\mathbf{\Gamma}}_\mathrm{x} = \mathbf{0}$, allowing the response covariance matrix to be obtained by solving the Lyapunov equation

$$\mathbf{A}_\mathrm{a}\mathbf{\Gamma}_\mathrm{x} + \mathbf{\Gamma}_\mathrm{x}\mathbf{A}_\mathrm{a}^\mathrm{T} + 2\mathbf{B}_\mathrm{a}\mathbf{S}_0\mathbf{B}_\mathrm{a}^\mathrm{T} = \mathbf{0} \tag{11}$$

The covariance of the structural output $\mathbf{y}$ can then be calculated via

$$\begin{aligned}\mathbf{\Gamma}_\mathrm{y} &= \mathbb{E}\left(\mathbf{y}\mathbf{y}^\mathrm{T}\right)\\ &= \mathbf{C}_\mathrm{a}\mathbf{\Gamma}_\mathbf{x}\mathbf{C}_\mathrm{a}^\mathrm{T}\end{aligned} \tag{12}$$

Therefore, if the moving load excitation can be represented as a filtered white noise, then the stochastic response of an arbitrary linear bridge structure can be determined directly. To this end, the next section proposes a filtered white noise approximation to represent the stochastic moving load.

3. Stochastic moving load model

This section describes the procedure for computing the filtered white noise representation of stochastic traffic loading. First, the load model for a single stream of loads, akin to a single traffic lane, is presented as a spatio-temporal random field of moving forces. Subsequently, the first and second order statistics, as well as the PSD, are derived; these results are illustrated for a rectangular pulse loading process. Finally, the load is discretized and converted to a vector random field that can be expressed as filtered white noise.

3.1. Load model

The load, which is shown schematically in Fig. 1, is modeled as a random field of spatial position x and time t, such that $0 \le x \le L$ and $t \ge 0$ and defined as the summation of $N(t)$ individual moving loads $f_i(x,t)$, i.e.,

$$f(x,t) = \sum_{i=1}^{N(t)} f_i(x,t) \tag{13}$$

$$f_i(x,t) = A_i h\left(x - v\left(t - t_i\right) + \epsilon\right) \tag{14}$$

where x is the location of the leading edge of the load function, $h(\cdot)$, which has a small constant width 2ϵ; L is the span length of the structure; A_i represents the load amplitude, which are positive random variables that are independent and identically distributed (i.i.d.) with mean μ_A and variance σ_A^2; t_i is the stochastic arrival time, which is independent of the load magnitude; and v is the velocity of the moving load, which is considered constant. This assumption of constant velocity is consistent with past approaches to this problem [4,9–12,15–17,19,27]. The stream of moving loads can be thought of as a single lane of traffic. It is assumed that the loading parameters are constant in time. The load function $h(z)$ is centered around $z = 0$ and is normalized such that

$$\int_{-\epsilon}^{\epsilon} h(z)\,dz = 1 \tag{15}$$

Assuming that the number of loads $N(t)$ is a Poisson counting process with constant arrival rate λ, then the process defined in Eqs. (13)–(14) is a compound Poisson process [29]. For a given number of loads $N(t) = n$, the compound Poisson process has the arrival times $t_1 < t_2 < \cdots < t_n$ which are independent and uniformly distributed on the interval $[0,t]$, i.e., the probability distribution function (PDF) $f_{t_i}(\tau)$ of each arrival time is

$$f_{t_i}(\tau) = \begin{cases} \dfrac{1}{t}, & \text{if } 0 \le \tau \le t \\ 0, & \text{otherwise} \end{cases} \tag{16}$$

3.2. Mean, auto-covariance, and PSD

The first and second moments, as well as the PSD, of the loading process are computed next. The expected value of the loading process, conditional on $N(t) = n$, is given by

$$\begin{aligned} \mathbb{E}\left[f(x,t)\,|N(t)=n\right] &= \sum_{i=1}^{n} \mathbb{E}\left[A_i h\left(x - v\left(t - t_i\right) + \epsilon\right)\right] \\ &= n\mu_A \mathbb{E}\left[h\left(x - v\left(t - t_i\right) + \epsilon\right)\right] \end{aligned} \tag{17}$$

Using Eq. (16), the expected value of the distribution is computed using the substitutions $d = x - vt + \epsilon$ and $z = d + vt_i$ as follows

$$\begin{aligned} \mathbb{E}\left[h\left(x - v\left(t - t_i\right) + \epsilon\right)\right] &= \int_0^t h\left(d + vt_i\right) f_{t_i}\left(t_i\right) dt_i \\ &= \frac{1}{tv}\int_{x-vt+\epsilon}^{x+\epsilon} h(z)\,dz \end{aligned} \tag{18}$$

For a sufficiently large value of t (in this case, $t > \frac{L+2\epsilon}{v}$) and noting that $\mathbb{E}[N(t)] = \lambda t$, the unconditional expected value of the loading is given by

$$\begin{aligned} \mathbb{E}[f(x,t)] &= \mathbb{E}\left[\mathbb{E}\left[f(x,t)\,|N(t)=n\right]\right] \\ &= \frac{\lambda\mu_A}{v} \end{aligned} \tag{19}$$

Because the stream of moving loads represents the physical vehicle traffic on the bridge (i.e., all forces are positive), the loading process has a nonzero positive mean, which is constant across the span of the bridge. A higher arrival rate indicates that more vehicles are on the span at any given time, resulting in a higher mean load. Conversely, for higher velocities, each load takes less time to cross the span, so at any given time the load is less likely to be on the span, resulting in a lower mean load.

The conditional correlation function of the loading process is defined for spatial and time coordinate pairs (x,t) and (y,s) where it is assumed that $s > t$; the independent increments property of the Poisson process is used.

$$\begin{aligned} &\mathbb{E}\left[f(x,t)\,f(y,s)\,|N(t)=n, N(s)-N(t)=m\right] \\ &= \sum_{i=1}^{n}\sum_{j=1}^{n+m} \mathbb{E}\left[f_i(x,t)\,f_j(y,s)\right] \end{aligned} \tag{20}$$

Here, index i is associated with (x,t) and j with (y,s) where $1 \le i \le n$ and $1 \le j \le n+m$. For the case where $i = j$

$$\begin{aligned} &\mathbb{E}\left[f_i(x,t)\,f_i(y,\mathrm{s})\right] \\ &= \mathbb{E}\left[A_i^2\right]\mathbb{E}\left[h\left(x - v\left(t - t_i\right) + \epsilon\right) h\left(y - v\left(s - t_i\right) + \epsilon\right)\right] \\ &= \frac{\left(\mu_A^2 + \sigma_A^2\right)}{vt} J(vt + d, e - d) \end{aligned} \tag{21}$$

where $e = y - vs + \epsilon$, and $e - d = (y - vs + \epsilon) - (x - vt + \epsilon) = \Delta x - v\tau$, and the function $J(\gamma,\alpha)$ is defined as

$$J(\gamma,\alpha) = \int_{-\epsilon}^{\gamma} h(z)\,h(z+\alpha)\,dz \tag{22}$$

Note that for sufficiently large value of t, in this case $t > \frac{L+2\epsilon}{v}$, when a load could have completely crossed the span and the random input process has reached stationarity, $d < -\epsilon$, and therefore $J(d, e-d) = 0$. For the case where $i \ne j$, these two forces are independent. Here it is assumed that $s > t$, where i is the index of loads $0 < i < n$ and j is the index of loads $0 < j < m + n$. The terms in Eq. (20) become

$$\begin{aligned} &\mathbb{E}\left[f_i(x,t)\,f_j(y,\mathrm{s})\,|N(t)=n, N(s)-N(t)=m\right] \\ &= \mathbb{E}\left[f_i(x,t)\,|n,m\right]\mathbb{E}\left[f_j(y,\mathrm{s})\,|n,m\right] \\ &= \begin{cases} 0 & \text{if } j \le n \\ \dfrac{1}{t(t-s)}\left(\dfrac{\mu_A}{v}\right)^2 & \text{if } j > n \end{cases} \end{aligned} \tag{23}$$

The double summation in Eq. (20) then needs to combine the n instances of $i = j$ plus the nm instances of $i \ne j$ where $j > n$ plus the $n^2 - n$ instances of $i \ne j$ where $j \le n$, yielding

$$\begin{aligned} &\mathbb{E}\left[f(x,t)\,f(y,s)\,|N(t)=n, N(s)-\mathrm{N(t)}=m\right] = \\ &(n)\left(\frac{\left(\mu_A^2+\sigma_A^2\right)}{vt} J(vt+d, e-d)\right) + \left(n^2-n\right)(0) + (nm)\left(\frac{1}{t(t-s)}\left(\frac{\mu_A}{v}\right)^2\right) \end{aligned} \tag{24}$$

Next the expected value is evaluated for the number of loads for the Poisson random variable $N(t)$ and $N(s)$, which recalling that $s > t$, becomes

$$\begin{aligned} \mathbb{E}\left[\mathrm{N(t)}\right] &= \lambda t \\ \mathbb{E}\left[N(t)^2\right] &= (\lambda t)^2 + \lambda t \\ \mathbb{E}\left[N(t)^2 - N(t)\right] &= (\lambda t)^2 \\ \mathbb{E}\left[N(t)\left(N(s) - N(t)\right)\right] &= \lambda^2(st - t^2) \end{aligned} \tag{25}$$

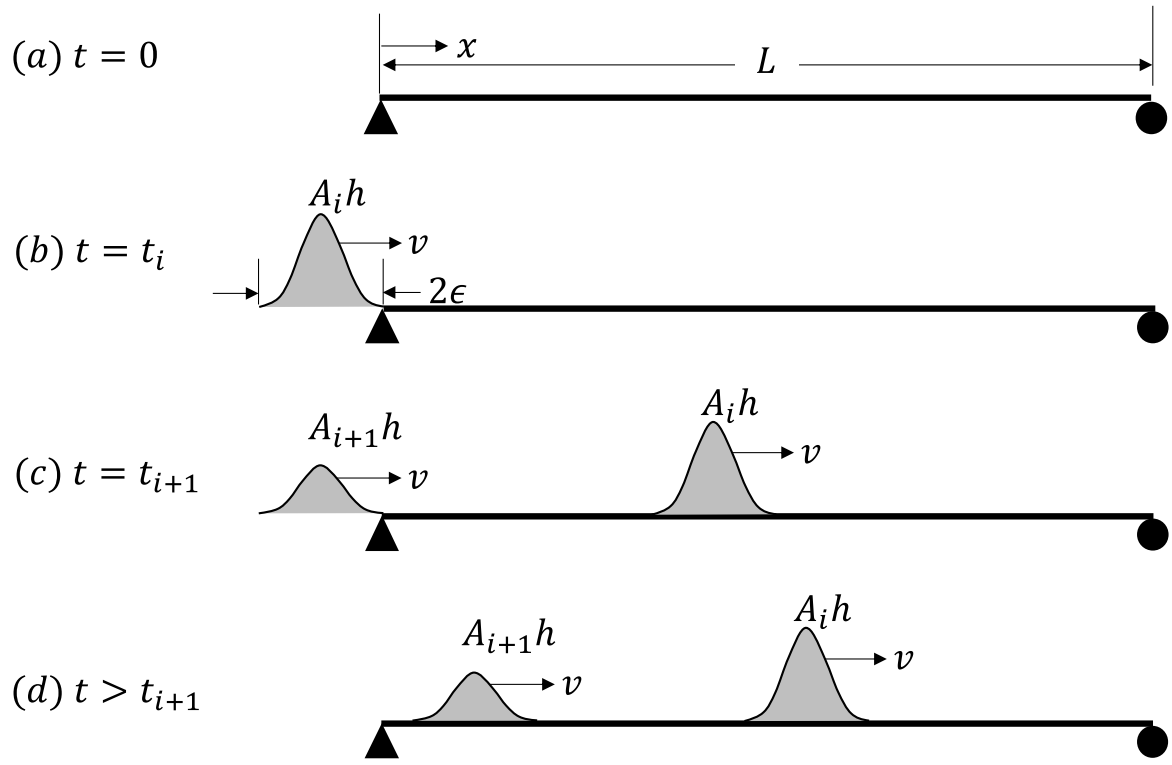

Fig. 1. Schematic of the moving load model. (a) at the initial time, no loads are present, (b) first load arrives at time $t = t_i$, (c) second load arrives at time $t = t_{i+1}$, and (d) loads moving along x as time increases.

These expectations are then used to compute the auto-correlation per the double summation of Eq. (20) as

$$\begin{aligned} R(\Delta x, \tau) &= \mathbb{E}[f(x,t) f(y,s)] \\ &= \frac{\lambda\left(\mu_A^2 + \sigma_A^2\right)}{v} J(x+\epsilon, \Delta x - v\tau) + \left(\frac{\lambda \mu_A}{v}\right)^2 \end{aligned} \tag{26}$$

where $\Delta x = x - y$, and $\tau = t - s$. The auto-covariance function is then computed as

$$\begin{aligned} K(\Delta x, \tau) &= \mathbb{E}[f(x,t) f(y,s)] - \mathbb{E}[f(x,t)]\,\mathbb{E}[f(y,s)] \\ &= \frac{\lambda\left(\mu_A^2 + \sigma_A^2\right)}{v} J(x+\epsilon, \Delta x - v\tau) \end{aligned} \tag{27}$$

Note that the auto-covariance function is a function of Δx and τ, which together with the fact that mean is constant, indicates that the random field is weakly homogeneous. The PSD of the loading is computed as the Fourier transform of the auto-covariance function in the variable τ

$$S(\Delta x, \omega) = \mathcal{F}(K(\Delta x, \tau)) \tag{28}$$

3.3. Rectangular pulse example

To illustrate the proposed approach, consider the case when the load is a rectangular pulse, i.e., constant over the region $z \in [-\epsilon, \epsilon]$, which results in

$$h(z) = \begin{cases} \frac{1}{2\epsilon} & \text{if } z \in [-\epsilon, \epsilon] \\ 0 & otherwise \end{cases} \tag{29}$$

The expected value computed using Eq. (19) is independent of the loading distribution, $\mathbb{E}[f(x,t)] = \frac{\lambda \mu_A}{v}$. The function $J(\gamma, \alpha)$ in Eq. (22) then becomes

$$J(\gamma, \alpha) = \begin{cases} 0 & \text{if } |\alpha| > 2\epsilon \\ \left[\frac{2\epsilon + \alpha}{4\epsilon^2} \quad \epsilon \le \gamma\right] & \text{if } -2\epsilon < \alpha \le 0 \\ \left[\frac{2\epsilon - \alpha}{4\epsilon^2} \quad \epsilon - \alpha \le \gamma\right] & \text{if } 0 < \alpha \le 2\epsilon \end{cases} \tag{30}$$

which, when evaluated at $\gamma = x + \epsilon$, and $\alpha = \Delta x - v\tau$, the result is:

$$J(x+\epsilon, \Delta x - v\tau) = \frac{2\epsilon - |\Delta x - v\tau|}{4\epsilon^2} \quad \text{if } -2\epsilon < \Delta x - v\tau < 2\epsilon \tag{31}$$

This result is a shifted triangular pulse, which is nonzero only for values of $\frac{-2\epsilon}{v} \le \tau - \frac{\Delta x}{v} \le \frac{2\epsilon}{v}$. The resulting auto-correlation where $i = j$ is computed from Eq. (21) as

$$\begin{aligned} \mathbb{E}\left[f_i(x,t) f_i(y,s)\right] &= \frac{\left(\mu_A^2 + \sigma_A^2\right)}{vT} J(x+\epsilon, \Delta x - v\tau) \\ &= \begin{cases} \frac{\left(\mu_A^2 + \sigma_A^2\right)}{(2\epsilon)^2 t}\left(\frac{2\epsilon}{v} - \left|\frac{\Delta x}{v} - \tau\right|\right) & \text{if } \frac{-2\epsilon}{v} \le \tau - \frac{\Delta x}{v} \le \frac{2\epsilon}{v} \\ 0 & \text{otherwise} \end{cases} \end{aligned} \tag{32}$$

and where $i \neq j$ from Eq. (23) $\mathbb{E}\left[f_i(x,t) f_j(y,s)\right] = \frac{1}{t(s-t)}\left(\frac{\mu_A}{v}\right)^2$ which is independent of the pulse shape. Combining these terms per Eq. (26) results in the auto-correlation

$$\begin{aligned} R(\Delta x, \tau) &= \mathbb{E}[f(x,t) f(y,s)] \\ &= \frac{\lambda\left(\mu_A^2 + \sigma_A^2\right)}{(2\epsilon)^2}\left(\frac{2\epsilon}{v} - \left|\frac{\Delta x}{v} - \tau\right|\right) + \left(\frac{\lambda \mu_A}{v}\right)^2 \end{aligned} \tag{33}$$

Subtracting the product of expected values results in the auto-covariance:

$$\begin{aligned} K(\Delta x, \tau) &= \mathbb{E}[f(x,t) f(y,s)] - \mathbb{E}[f(x,t)]\,\mathbb{E}[f(y,s)] \\ &= \begin{cases} \frac{\lambda\left(\mu_A^2 + \sigma_A^2\right)}{(2\epsilon)^2}\left(\frac{2\epsilon}{v} - \left|\frac{\Delta x}{v} - \tau\right|\right) & \text{if } \frac{-2\epsilon}{v} \le \tau - \frac{\Delta x}{v} \le \frac{2\epsilon}{v} \\ 0 & \text{otherwise} \end{cases} \end{aligned} \tag{34}$$

Then the power spectral density is

$$\begin{aligned} S(\Delta x, \omega) &= \mathcal{F}(K(\Delta x, \tau)) \\ &= \frac{\lambda\left(\mu_A^2 + \sigma_A^2\right)}{2\pi v^2} e^{-i\omega \frac{\Delta x}{v}} \operatorname{sinc}^2\left(\frac{\epsilon \omega}{v}\right) \end{aligned} \tag{35}$$

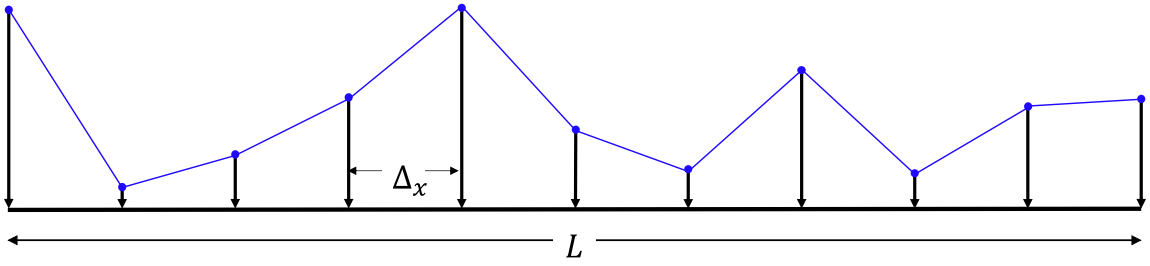

Fig. 2. Schematic of spatial discretization of stochastic moving loads with linear interpolation.

In terms of dimensions, this PSD evaluates to $\left(\frac{force}{distance}\right)^2 \frac{1}{\text{Hz}}$ as expected for a distributed loading process. In the limit as ϵ approaches zero, i.e., the loading width is negligible compared to the length of the bridge, then

$$S(\Delta x, \omega) = \frac{\lambda\left(\mu_A^2 + \sigma_A^2\right)}{2\pi v^2} e^{-i\omega\frac{\Delta x}{v}} \tag{36}$$

For this case, note that the magnitude of the PSD is constant for all frequencies

$$\begin{aligned} S(0,\omega) &= \frac{\lambda\left(\mu_A^2 + \sigma_A^2\right)}{2\pi v^2}, \\ |S(\Delta x, \omega)| &= \frac{\lambda\left(\mu_A^2 + \sigma_A^2\right)}{2\pi v^2} \end{aligned} \tag{37}$$

Whether the width of uniformly distributed moving loads could be considered to be negligible can be determined by examining the magnitude of $\text{sinc}^2\left(\frac{\epsilon\omega}{v}\right)$ in Eq. (35); if $\text{sinc}^2\left(\frac{\epsilon\omega}{v}\right)$ is sufficiently close to 1.0 over the frequency range of interest, then the loading width can be considered negligible, i.e., the loads can be considered as point loads and Eqs. (36)–(37) hold. If the loading were initially considered as point loads rather than as distributed loads, a derivation of the loading PSD, as shown in Appendix A, produces the same result obtained here as ϵ goes to zero.

4. State space representation for the stochastic moving load model

This section shows how the loading derived in Section 3 can be represented in state space form given in Eq. (4). First, the spatially continuous stochastic random field $f(x,t)$ is discretized in space. Then, a rational approximation of the complex exponential term of the PSD is developed. Subsequently, a single state space system with a white noise input is obtained, whose output corresponds to the discretized random field. This system is then reduced via balanced reduction to enable a more efficient solution of the Lyapunov equation. It is worth noting that other white noise representations of stochastic traffic can also be considered here, such as those presented by Ditlevsen and Madsen [27,28] after a modification to account for constant traffic velocity.

4.1. Discretization of the continuous random field

First, the random field $f(x,t)$ is discretized in space assuming a piecewise linear spatial variation [30], as shown in Fig. 2, where the vector random process $\mathbf{f}(t)$ defined as

$$\mathbf{f}(t) = \left[f_{x_1}(t), f_{x_2}(t), \ldots, f_{x_{N_\text{d}}}(t)\right]^\text{T} \tag{38}$$

where x_j corresponds to the loading discretization points, and N_d is the number of input points. This discretization represents the continuous loading as

$$f(x,t) = \sum_{k=1}^{N_d} f_{x_k}(t)\,\phi_k(x) \tag{39}$$

where $f_{x_k}(t)$ is the point load temporal process at location x_k, and $\phi_k(x)$ is the spatial contribution from location x_k. Using a linear interpolation between loaded points results in

$$\phi_k(x) = \begin{cases} 1 - \left|\frac{x_k - x}{\Delta_x}\right| & \text{if } x_k - \Delta_x \le x \le x_k + \Delta_x \\ 0 & otherwise \end{cases} \tag{40}$$

where Δ_x is the spacing between adjacent discretization points.

Then, the mean of the vector random process is given by

$$\mathbb{E}[\mathbf{f}(t)] = \mathbb{E}[f(x,t)]\,\Delta_\text{x} = \frac{\mu_A \lambda}{v}\Delta_\text{x} \tag{41}$$

where Δ_x is the spacing between the discretized load points. The discretized mean load can be interpreted as a load distributed uniformly across the span, so the equivalent discretized loads are this distributed load collected over each tributary width. This discretized mean load can be computed from Eq. (39) with a constant for the force $f(x,t)$. The auto-covariance matrix function of the vector random process is then given by

$$K_{j,j+n}(\tau) = \begin{cases} \frac{\lambda}{v^2}\delta\left(\frac{n\Delta_x}{v} - \tau\right)\left(\mu_A^2 + \sigma_A^2\right) & \text{if } \epsilon = 0 \\ \frac{\lambda}{(2\epsilon)^2}\left(\mu_A^2 + \sigma_A^2\right)\left(\frac{2\epsilon}{v} - \left|\frac{n\Delta_x}{v} - \tau\right|\right) & \text{if } \epsilon > 0 \end{cases} \tag{42}$$

for point loads or distributed loads respectively. Here the matrix indices are given in relative terms $(j, j+n)$ since the values depend only on the difference between indices, n. The same is true for the PSD matrix of the vector random process is given by

$$S_{j,j+n}(\omega) = \begin{cases} \frac{\lambda\left(\mu_A^2 + \sigma_A^2\right)}{2\pi v^2} e^{-i\omega\frac{n\Delta_x}{v}} & \text{if } \epsilon = 0 \\ \frac{\lambda\left(\mu_A^2 + \sigma_A^2\right)}{2\pi v^2} e^{-i\omega\frac{n\Delta_x}{v}}\,\text{sinc}^2\left(\frac{\epsilon\omega}{v}\right) & \text{if } \epsilon > 0 \end{cases} \tag{43}$$

for point loads or distributed loads respectively. Note that for all frequencies, the diagonal entries (i.e., terms with $n = 0$) of the point loading PSD are constant and equal to $\frac{\lambda\left(\mu_A^2+\sigma_A^2\right)}{2\pi v^2}$ and all entries have constant magnitude and equal to $\frac{\lambda\left(\mu_A^2+\sigma_A^2\right)}{2\pi v^2}$. Also, $\frac{n\Delta_x}{v}$ corresponds to the positive time delay for the load to move from point x_j to point x_{j+n}. The PSD matrix in Eq. (43) can be factored as follows

$$S_{jk}(\omega) = S_0 H_j(\omega) H_k^*(\omega) \tag{44}$$

where $*$ is the complex conjugate, and $H_j(\omega)$ is given by

$$H_j(\omega) = \begin{cases} e^{-i\omega\frac{x_j}{v}} & \text{if } \epsilon = 0 \\ e^{-i\omega\frac{x_j}{v}}\,\text{sinc}\left(\frac{\epsilon\omega}{v}\right) & \text{if } \epsilon > 0 \end{cases} \tag{45}$$

and

$$S_0 = \frac{\lambda\left(\mu_A^2 + \sigma_A^2\right)}{2\pi v^2} \tag{46}$$

Then, the PSD matrix can be written in matrix form as

$$\mathbf{S}(\omega) = S_0 \mathbf{H}(\omega)\mathbf{H}^{\mathrm{H}}(\omega) \tag{47}$$

where $^{\mathrm{H}}$ is the Hermitian or complex conjugate transpose.

The exponential terms in the expression for $\mathbf{H}(\omega)$ in Eq. (45) requires an infinite-dimensional filter, which is not physically realizable [31,32]. The next section presents an approach using the Padé approximation to obtain a finite dimensional filter for $\mathbf{H}(\omega)$.

4.2. Padé approximation

To represent the loading in state space form, the term $e^{-s\tau}$ needs to be expressed as a rational polynomial function, where τ is the delay time and s is the Laplace variable. Note that the magnitude of the complex exponential $e^{-s\tau}$ is constant and equal to 1 for all frequencies, while the phase varies linearly, with a slope of τ. The Padé approximation is often used to represent $e^{-s\tau}$, as it also has a unit magnitude and linear phase over a bandwidth that depends on the number of terms taken in the approximation.

For a unit delay, $\tau = 1$, the Padé approximation is given by

$$e^{-s} = \frac{N_{p,q}(s)}{D_{p,q}(s)} \tag{48}$$

where $N_{p,q}$ and $D_{p,q}$ are polynomials of degree p and q, respectively. Typically, $p = q$, which ensures the magnitude is unity for all frequencies and the polynomials are given by

$$\begin{aligned} N_{q,q}(s) &= \sum_{j=0}^{q} \frac{(2q-j)!q!}{(2q)!j!(q-j)!}(-s)^j \\ D_{q,q}(s) &= \sum_{j=0}^{q} \frac{(2q-j)!q!}{(2q)!j!(q-j)!}s^j \end{aligned} \tag{49}$$

For an arbitrary delay τ, i.e., $e^{-\tau s}$, the numerator and denominator are given by $N_{p,q}(\tau s)$ and $D_{p,q}(\tau s)$, respectively. As shown in Fig. 4 for the simply supported beam example, the approximation order determines the bandwidth over which the phase is linear for a specific time delay.

4.3. Computing Padé approximants

Computing high order Padé approximants can be numerically challenging. To avoid numerical issues, the poles and zeros of the approximants can be computed directly, resulting in an accurate representation of high order systems [33]. For a unit delay, the poles $p_1, p_2, \ldots, p_q$ are obtained by solving the following system of nonlinear equations

$$f_k^{\mathrm{p}} = -\frac{1}{2} - \frac{p+q}{2p_k} + \sum_{j\neq k}\frac{1}{p_k - p_j} = 0 \tag{50}$$

where $k = 1, 2, \ldots, q$. Likewise, the zeros $z_1, z_2, \ldots, z_p$ are obtained by solving the following system of nonlinear equations

$$f_k^{\mathrm{z}} = \frac{1}{2} - \frac{p+q}{2z_k} + \sum_{j\neq k}\frac{1}{z_k - z_j} = 0 \tag{51}$$

where $k = 1, 2, \ldots, p$. The previous expressions are satisfied by the numerator and denominator polynomials, because of known properties for the roots of hypergeometric functions [33–35]. Each system of nonlinear equations is solved using Newton's method, where the gradients are computed in closed-form. An initial guess for the iterative method consists of points arranged in a left half ellipse for the poles and right half ellipse for the zeros [33]. Because the complex roots appear in conjugate pairs, this constraint is directly enforced in the solution to guarantee a real system. The phase angles used for determining Padé accuracy shown in Fig. 4 are also computed using this approach.

The poles $p_1, p_2, \ldots, p_q$ and zeros $z_1, z_2, \ldots, z_p$ are computed for a unit delay. Then for a delay d, the poles are equal to $p_1/d, p_2/d, \ldots, p_q/d$ and the zeros are equal to $z_1/d, z_2/d, \ldots, z_p/d$. The gain of the system is given as

$$g = \frac{q!(-1)^p}{p!d^{q-p}} \tag{52}$$

The system is constructed from the poles, zeros and gains, for example using the Matlab function *zpk*, and then converted directly to state space format. Using the transfer function should be avoided to reduce numerical errors.

4.4. State space representation of loading filter

To employ this filtered white noise loading system on a structural model, m separate subsystems must be created corresponding to the discretization of the random field. Then, the assembled loading system has one input and m outputs. The loading system assembly is

$$\begin{aligned} \mathbf{A}_{\mathrm{F}} &= \begin{bmatrix} \mathbf{A}_{\mathrm{f}1} & & & \\ & \mathbf{A}_{\mathrm{f}2} & & \\ & & \ddots & \\ & & & \mathbf{A}_{\mathrm{f}m} \end{bmatrix} \quad \mathbf{B}_{\mathrm{F}} = \begin{bmatrix} \mathbf{B}_{\mathrm{f}1} \\ \mathbf{B}_{\mathrm{f}2} \\ \vdots \\ \mathbf{B}_{\mathrm{f}m} \end{bmatrix} \\ \mathbf{C}_{F} &= \begin{bmatrix} \mathbf{C}_{\mathrm{f}1} & & & \\ & \mathbf{C}_{\mathrm{f}2} & & \\ & & \ddots & \\ & & & \mathbf{C}_{\mathrm{f}m} \end{bmatrix} \quad \mathbf{D}_{\mathrm{F}} = \begin{bmatrix} \mathbf{D}_{\mathrm{f}1} \\ \mathbf{D}_{\mathrm{f}2} \\ \vdots \\ \mathbf{D}_{\mathrm{f}m} \end{bmatrix} \end{aligned} \tag{53}$$

where each subsystem $\mathbf{A}_{\mathrm{f}i}$, $\mathbf{B}_{\mathrm{f}i}$, $\mathbf{C}_{\mathrm{f}i}$, $\mathbf{D}_{\mathrm{f}i}$ corresponds to the Padé delay for the ith discretized force in the random field, i.e., each subsystem is the state space realization of the Padé delay for the load to reach a specific input location. The fully assembled system is the white noise filter shown in Eq. (4).

The resulting assembled system, with matrices $\mathbf{A}_{\mathrm{F}}$, $\mathbf{B}_{\mathrm{F}}$, $\mathbf{C}_{\mathrm{F}}$, $\mathbf{D}_{\mathrm{F}}$, can be quite large, depending on the discretization of the random field and the order of the Padé approximations required. Balanced reduction is applied [36] prior to assembly of the augmented system, making the state space representation of the loading model more tractable.

4.5. Extension to multiple loading processes (Multiple traffic lanes)

This procedure can be expanded to consider multiple lanes of traffic, including vehicles moving in the opposite direction or with different velocities. In this case the sign of the time delay is reversed, and the PSD matrix is given by

$$S'_{j,j+n}(\omega) = \begin{cases} \dfrac{\lambda\left(\mu_A^2 + \sigma_A^2\right)}{2\pi v^2} e^{i\omega\frac{n\Delta_x}{v}} & \text{if } \epsilon = 0 \\ \dfrac{\lambda\left(\mu_A^2 + \sigma_A^2\right)}{2\pi v^2} e^{i\omega\frac{n\Delta_x}{v}} \operatorname{sinc}^2\left(\dfrac{\epsilon\omega}{v}\right) & \text{if } \epsilon > 0 \end{cases} \tag{54}$$

Instead of realizing positive delays using the Padé approximation, the coordinates can be redefined as $x'_i = L - x_i$, then

$$n\Delta_x = x_j - x_{j+n} = x_j - L + L - x_{j+n} = x'_{j+n} - x'_j = n\Delta'_x \tag{55}$$

Then, the PSD matrix is rewritten as

$$S_{j,j+n}(\omega) = \begin{cases} \dfrac{\lambda\left(\mu_A^2 + \sigma_A^2\right)}{2\pi v^2} e^{-i\omega\frac{n\Delta'_x}{v}} & \text{if } \epsilon = 0 \\ \dfrac{\lambda\left(\mu_A^2 + \sigma_A^2\right)}{2\pi v^2} e^{-i\omega\frac{n\Delta'_x}{v}} \operatorname{sinc}^2\left(\dfrac{\epsilon\omega}{v}\right) & \text{if } \epsilon > 0 \end{cases} \tag{56}$$

and

$$\mathbf{H}'(\omega) = \begin{cases} \left[e^{-i\omega\frac{L-x_1}{v}}, \ldots, e^{-i\omega\frac{L-x_{N_{\mathrm{d}}}}{v}}\right]^{\mathrm{T}} & \text{if } \epsilon = 0 \\ \left[e^{-i\omega\frac{L-x_1}{v}} \operatorname{sinc}\left(\dfrac{\epsilon\omega}{v}\right), \ldots, e^{-i\omega\frac{L-x_{N_{\mathrm{d}}}}{v}} \operatorname{sinc}\left(\dfrac{\epsilon\omega}{v}\right)\right]^{\mathrm{T}} & \text{if } \epsilon > 0 \end{cases} \tag{57}$$

to obtain

$$\mathbf{S}'^{(\omega)} = S_0 \mathbf{H}'^{(\omega)} \mathbf{H}'^{\mathrm{H}}(\omega)$$
$$S_0 = \frac{\lambda\left(\mu_A^2 + \sigma_A^2\right)}{2\pi v^2} \tag{58}$$

where S_0 is the intensity of the white noise process for this lane. As indicated here, the proposed method can be applied for reversed direction traffic but using spatial coordinates $L - x_1, L - x_2, \ldots, L - x_n$. First, assuming two independent streams of moving loads, one in each direction, the random field loading is given by

$$f(x,t) = f^+(x,t) + f^-(x,t) \tag{59}$$

where superscripts imply the moving direction, f^+ are the loads moving in the positive direction and f^- are the loads moving in the reverse direction. If these two processes have the same parameters (arrival rate λ, loading μ_A, σ_A and velocity v) then, $S_0^+ = S_0^-$ and the mean of the combined process discretized in space is given by

$$\mathbb{E}[\mathbf{f}(t)] = \frac{2\mu_A \lambda}{v} \Delta_x \tag{60}$$

Assuming the processes are independent, the auto-covariance function is the sum of the auto-covariance function of each process. Because of the linear property of the Fourier transform, then, the PSD of the combined process is the sum of the PSD for each traffic lane, i.e.,

$$S(\Delta x, \omega) = S^+(\Delta x, \omega) + S^-(\Delta x, \omega) \tag{61}$$

where S, S^+, and S^- represent the PSD for the combined loads, loads moving in positive direction, and loads moving in reverse direction, respectively. Similarly, after the discretization,

$$\begin{aligned}\mathbf{S}(\omega) &= \mathbf{S}^+(\omega) + \mathbf{S}^-(\omega) \\ &= S_0^+ \mathbf{H}^+(\omega)\left(\mathbf{H}^+(\omega)\right)^{\mathrm{H}} + S_0^- \mathbf{H}^-(\omega)\left(\mathbf{H}^-(\omega)\right)^{\mathrm{H}}\end{aligned} \tag{62}$$

Then, the following expression is obtained

$$\mathbf{S}(\omega) = \begin{bmatrix}\mathbf{H}^+(\omega) & \mathbf{H}^-(\omega)\end{bmatrix} \mathbf{S_0} \begin{bmatrix}\mathbf{H}^+(\omega) & \mathbf{H}^-(\omega)\end{bmatrix}^{\mathrm{H}} \tag{63}$$

The previous expression implies that the excitation system has now two inputs and the same number of outputs. Here, $\mathbf{S_0}$ is the PSD matrix of the two input processes. Assuming they are uncorrelated, this is a diagonal matrix with entries of S_0^+ and S_0^-. Furthermore, if a uniform spatial discretization is used, then, $H_i^- = H_{N_d+1-i}^+$, i.e., $\mathbf{H}^-$ is equal to $\mathbf{H}^+$ but reversing the order of the entries.

The traffic model can be extended readily to any number of lanes in both directions. Note however that when assembling the state space representation, the time delay, $\frac{n\Delta_x}{v}$, for a load moving from left to right is based on the distance from the left end of the span to a given input point, and the time delay for a load moving from right to left, $\frac{n\Delta_x}{v}$, is based on the distance from the right end to that same input point, these will be different delays, therefore requiring different Padé approximations.

5. Numerical examples

This section presents two numerical examples to demonstrate the efficacy of the proposed loading model. For comparison with previously proposed loading models, a simply supported beam is examined for various loading speeds. The results at midspan are used here to compare the temporal response magnitudes. The second example considers a more complex three-span truss with flexible interior supports. In this case, multiple modes are necessary to sufficiently characterize the structure's response. This example demonstrates the accuracy of the spatial response covariance, as well as member force results, and the application of the same loading system to multiple structural configurations. For comparison purposes, response variances are compared with numerical simulation, modal superposition (discussed further in Appendix B), and the frequency domain approach [20].

Table 1
Structure and loading parameters used in the simply supported beam example.

Description		Parameter	Value	Units
Structural parameters	Span length	L	20	m
	Flexural stiffness	EI	200e3	kN m^2
	Mass density	ρ	2500	kg/m^3
	Damping	ζ	0.02	–
Loading parameters (Uniform distribution)	Poisson arrival rate	λ	10	1/s
	Mean load magnitude	μ_A	44.5	kN
	Variance of load magnitude	σ_A^2	26.38	kN^2
	Load range	$A_{max} - A_{min}$	17.8	kN
	Load velocity	v	varies	m/s
	Mean load	$\mathbb{E}[f(x,t)] = \frac{\mu_A \lambda}{v}$	varies	kN/m

5.1. Simply supported beam example

The first example consists of a simply supported beam which is representative of simply supported bridge structures. Fig. 3 shows a schematic of the example, and Table 1 lists the parameters considered. The dynamic displacement response of a simply supported beam is largely governed by a single mode, i.e., a single degree-of-freedom assumed modes model, Eq. (72) with $n = 1$. However, to achieve better results for midspan velocity and acceleration, a model including the first five modes is used. For this structural model, the load effects matrix, $\mathbf{G}$ from Eq. (1) is defined as

$$G_{ij} = \int_{x_j - \Delta_x}^{x_j + \Delta_x} \psi_i(z)\, \phi_j(z) dz \tag{64}$$

for structural dof i and loading discretization j. In a finite element formulation, $\psi_i(x)$ is the element shape functions corresponding to dof i. In an assumed modes formulation $\psi_i(z)$ is the ith assumed mode shape which does not necessarily need to be the same as a natural mode of the structure. The loading discretization is considered in $\phi_j(z)$ as a linear interpolation between discrete load points as shown in Eq. (40). After computing the state space representation of the structure, its modal frequencies are used to determine an upper frequency target for computing the Padé approximation of the loading systems.

The span length of 20 m and load velocity of 25 m/s result in a time of 0.8 s for the load to cross the span. In computing the Padé approximates for this example, a 0.8 s delay is required for the longest delay system. A comparison of polynomial order and Padé accuracy for a 0.8 s delay is shown in Fig. 4. If only the first mode behavior is needed to represent the entire response, then an order smaller than 10 is adequate for the longest delay Padé approximation. However, when the response of the first five modes is required, an 80th order polynomial is required.

The response variance computed using the proposed approach is dependent on the number of input locations. This convergence behavior is somewhat dependent on the structure and loading parameters and should be investigated for a given set of parameters to determine an acceptable number of loading points, similar to a mesh sensitivity study for determining the appropriate mesh discretization used when building a FE model. Results shown here use 48 equal sized regions, $\Delta_x = 0.417$ m for applying the loading to the model as further refinement results in less than 1% change in results.

Results of the proposed approach are compared with traditional methods in Figs. 5 through 7. Fig. 5 compares the temporal average of 1000 simulations with the proposed method's mean response. In this example, the excitation is stationary, but the response requires some time from initiation of the loading until stationarity due to the initial conditions. Fig. 6 shows the ensemble variance for the midspan displacement, velocity and acceleration, across 1000 simulations comparing to modal superposition, the frequency domain method and the proposed approach. Note that this figure presents the solution of the

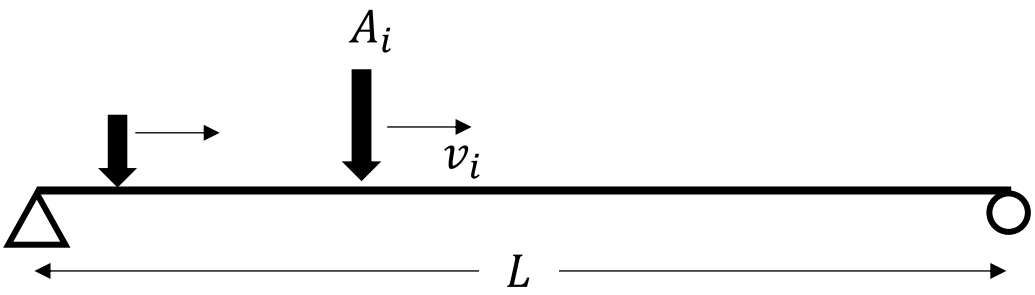

Fig. 3. Schematic of simply supported beam example.

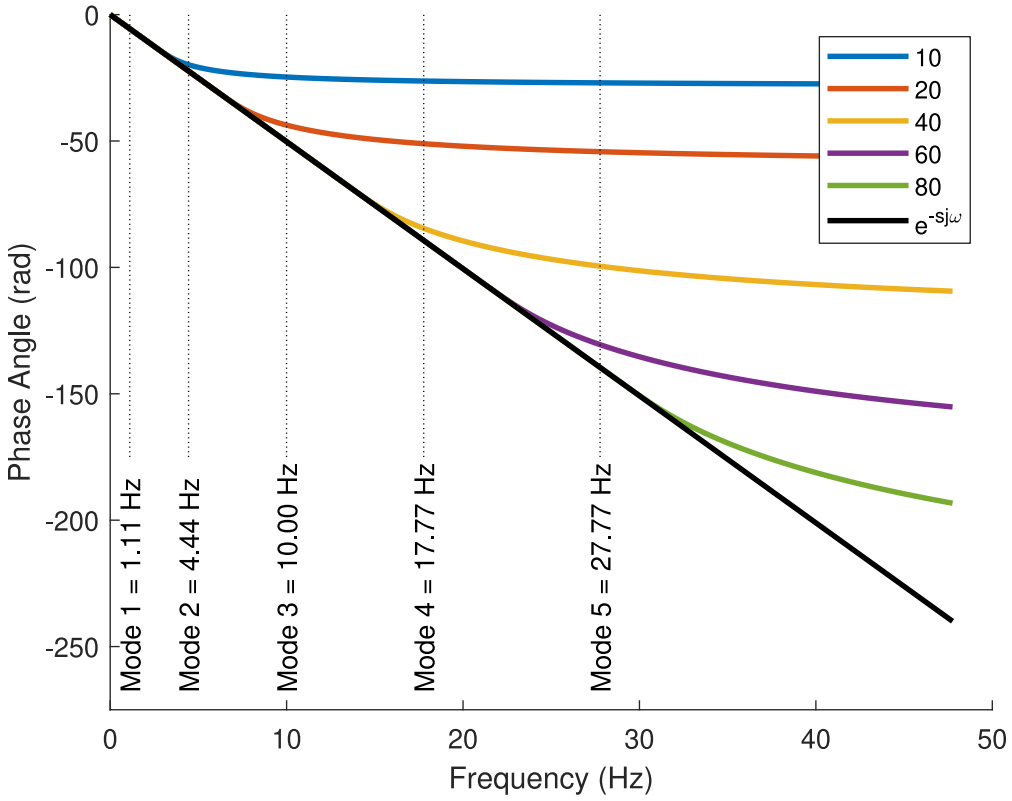

Fig. 4. Padé approximant accuracy for a 0.8 s delay using different polynomial orders.

differential Lyapunov equation [20] which converges to the stationary response in time. Nearly all of the displacement and velocity response, and 90% of the acceleration response, is from the first mode.

Fig. 7 shows the nondimensional stationary displacement variance, ς^2, vs. the nondimensional moving load velocity, α, which are given by

$$\varsigma^2 = \sigma^2 \frac{\left(\rho L \omega_1^2\right)^2}{\mathbb{E}[A^2]} \tag{65}$$

$$\alpha = \frac{v}{v_{cr}} = \frac{v}{2 f_1 L} \tag{66}$$

where v_{cr} is the velocity which equates the time required to cross the span, $\frac{L}{v}$, with half of the first fundamental period of the structure, $\frac{T_1}{2} = \frac{1}{2f_1}$ [10,37].

As it can be observed, the mean and variance of the responses calculated with the proposed method compares well with those from numerical simulations and alternative methods.

5.2. Three-span truss example

The second example is a three-span truss bridge. The intent of this example is to demonstrate the proposed method's stationary spatial output, as well as the ability to use the same loading system on varying structural configurations. A schematic of the truss considered is shown in Fig. 8. The bridge has a total length of 300 m, with three equal spans of 100 m each. This planar truss consists of 117 pin-connected members, all with equal area. The material density has been artificially increased to account for components not included in the model, such as floor system, decking, barriers etc. A full list of model parameters is shown in Table 2. The interior supports are modeled with springs to enable studying the effects of varying support stiffness on the stochastic responses. In this example, both displacement and truss axial force results are compared. The discretization of the loading required for accurate results varies depending on the output quantity being considered. Figs. 9 and 10 present the convergence of displacement variance and member axial force standard deviation, respectively, for varying number of input discretizations. Each line in Fig. 9 corresponds

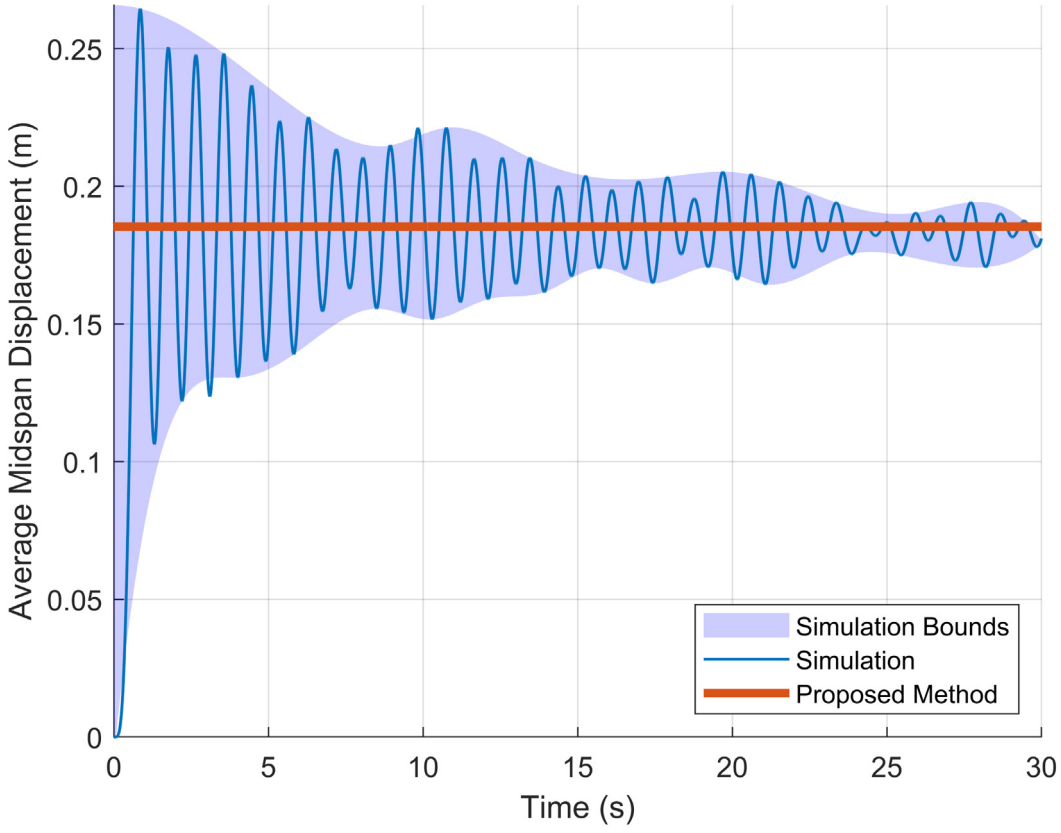

Fig. 5. Midspan displacement mean responses. Simulation ensemble mean and theoretical mean $= \frac{5w_\mu L^4}{384EI}$ where $w = \frac{\mu_A \lambda}{v}$.

Table 2
Structure and loading parameters used in the three-span truss example.

Description		Parameter	Value	Units
Structural parameters	Span length	L	100	m
	Truss height	H	10	m
	Member axial stiffness	EA	6.3e6	kN
	Mass density	ρ	10×7850	kg/m^3
	Support spring stiffness	k_{s1}, k_{s2}	1e12	N/m
	Damping	ζ	0.04	–
Loading parameters (Uniform Distribution)	Poisson arrival rate	λ	10	1/s
	Mean load magnitude	μ_A	44.5	kN
	Variance of load magnitude	σ_A^2	26.38	kN^2
	Load range	$A_{max} - A_{min}$	17.8	kN
	Load velocity	v	25	m/s
	Mean load	$\mathbb{E}[f(x,t)] = \frac{\mu_A \lambda}{v}$	17.8	kN/m

to a node on the bottom chord, and each line in Fig. 10 corresponds to a truss member, excluding the zero force members. In these figures, the response variance is normalized by the result from the smallest discretization to allow all outputs to be interpreted simultaneously. A flat line at 1.0 as the discretizations get smaller indicates results have converged.

From these figures, it is clear that the axial force results require a finer loading discretization than the displacements. For all results presented in this section, the smaller loading increment of 1.5 m (200 points in 300 m) is used.

The nodal displacement variances of bottom chord nodes are compared to simulation in Fig. 11 and the full covariance matrices are compared in Fig. 12. These results show a good agreement between methods. The proposed method is within 4% of the simulation results with the best match being along the diagonal, i.e., the auto-covariance terms.

The member axial force results are presented in terms of standard deviation in Fig. 13. Most truss members show a very good agreement between methods, within 5% of simulation results. Note that the zero force members are excluded from Fig. 13 as they have very low magnitude responses, which makes quantifying error problematic.

Next, one of the main advantages of the proposed method, efficient computing of the responses for multiple structural configurations, is compared to other approaches. In the proposed approach, the same loading system is considered for each configuration, where alternative approaches would require re-computing the coupled loading and structural terms, i.e., the mode shape dependent loading in the modal superposition approach. Fig. 14 presents the displacement variance of bottom chord nodes for three variations of the truss geometry, in each case the proposed method compares well with the simulation results. Finally, in Fig. 15, multiple values of the support stiffness k_{s1} (shown in Fig. 8) are evaluated while k_{s2} remains unchanged. Again, each evaluation uses the same loading system, so solving for response variance requires only solving the Lyapunov equation for the new augmented system as shown in Eq. (11).

As can be observed, the responses calculated using the proposed method are in good agreement with the responses from conventional approaches. Furthermore, this example highlights the advantages of the method for efficiently computing the response under varying structural configurations.

6. Conclusions

Modeling the dynamic process of random vehicles moving across a bridge is complex, and solving for the associated stochastic responses is challenging. Often, the vehicle loading is idealized as a compound Poisson process, that is, as a stream of randomly occurring loads of

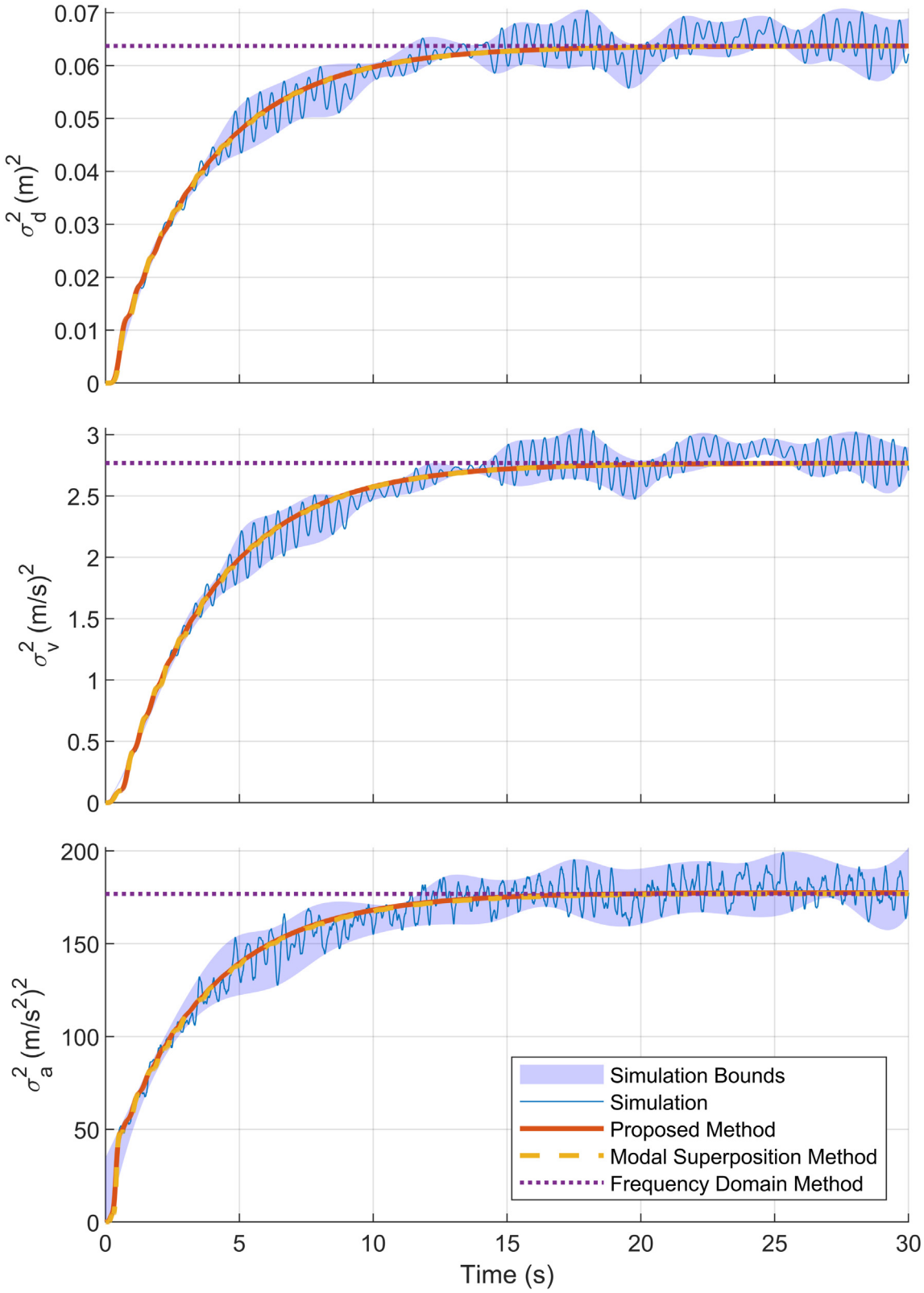

Fig. 6. Midspan displacement, velocity and acceleration variance from initiation until stationarity, computed with different methods. ($\lambda = 10$, Frequency domain method provides stationary response variance.)

random magnitude and constant velocity. Traditional approaches to solve for the corresponding structural responses represent the loading process in terms of the modes of the structure, and thus couple the loading with the structure to which it is applied. To address this issue, this paper presents an approach in which the discrete stochastic moving load is approximated as a filtered white noise.

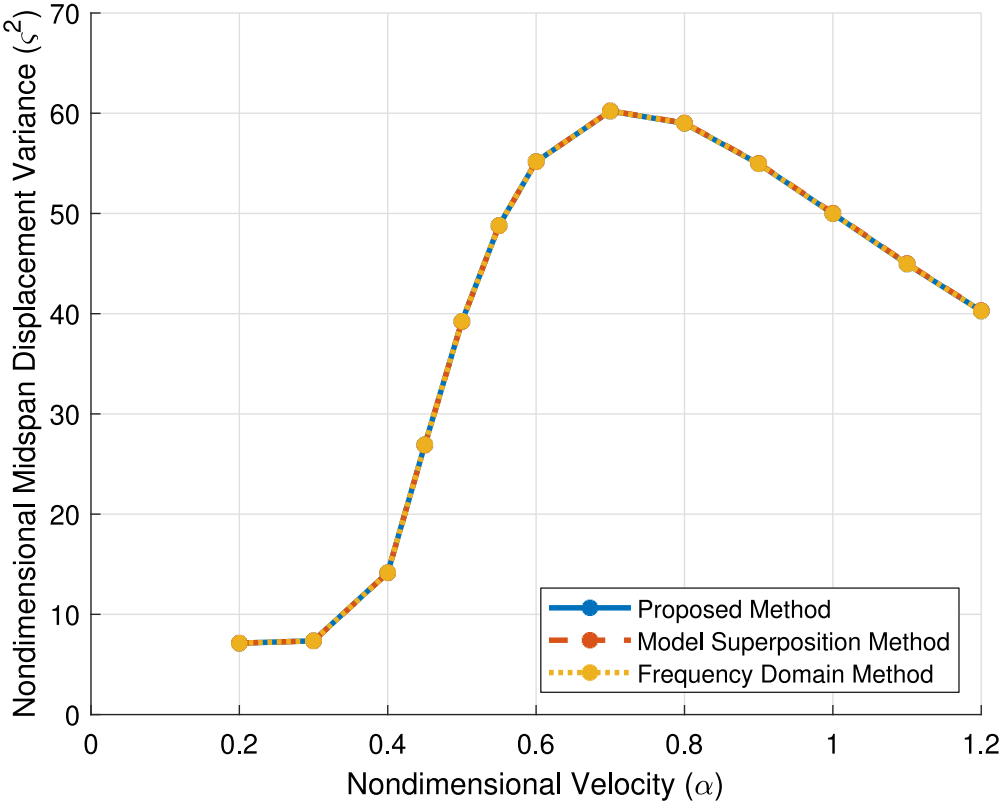

Fig. 7. Nondimensional midspan stationary displacement variance as a function of nondimensional velocity. (Matches results shown in Fig. 9 of Zibdeh and Rackwitz [37]).

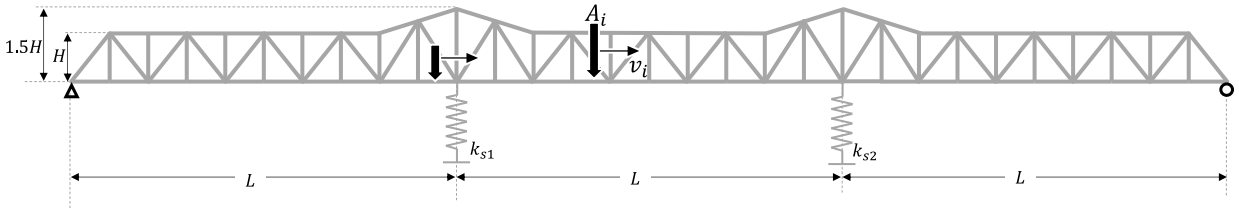

Fig. 8. Three-span truss schematic.

First, the loading process was separated into a nonzero static mean load and a stochastic dynamic component. The PSD of the stochastic component was derived as a function of the stochastic load parameters and the distance between discretized points in the form of a complex exponential. To represent this load process as a filtered white noise, the complex exponential was approximated as a ratio of polynomials using Padé approximants. These polynomials were realized in a state space system for each point along the bridge and assembled into a single-input multiple-output loading system. The result was a state space filter that converts the continuous white noise input to a spatially discretized approximation of the stochastic moving load process. To increase computational efficiency, balanced reduction was applied, prior to combining with the state space model of the structure to create an augmented system. Then, the response variances of the bridge were computed via the Lyapunov equation. The approach was shown to closely approximate the discrete Poisson process loading through comparison of responses for two example structures.

The first example was a simply supported beam that showed the relationship between the Padé approximation order and the target frequency of the loading system. Additionally, this benchmark example demonstrated that the temporal behavior of the response variances using this approach match those of existing solutions in the literature. The second example considered a more complex three-span truss bridge to demonstrate the spatial displacement covariance results, as well as truss member force results, both of which compare well with simulation. This example was also used to demonstrate the flexibility of the proposed approach by analyzing variations of the structure using the same loading system. These examples confirmed that the solution computed with the proposed method is in excellent agreement with other solution methods, including modal superposition, Monte Carlo simulation, and the frequency domain method. The second example also demonstrated the convergence of the proposed method as a function of the loading discretization. Note that when considering longer delay times between locations or higher target frequencies, higher-order Padé approximations are required. This can lead to very large loading systems and more computational time. However, this system only needs to be computed once and can be applied to different structural configurations, so long as the same traffic parameters and loading discretization are employed and the frequency target is still applicable. In the three-span truss example, the proposed method for computing response variances took

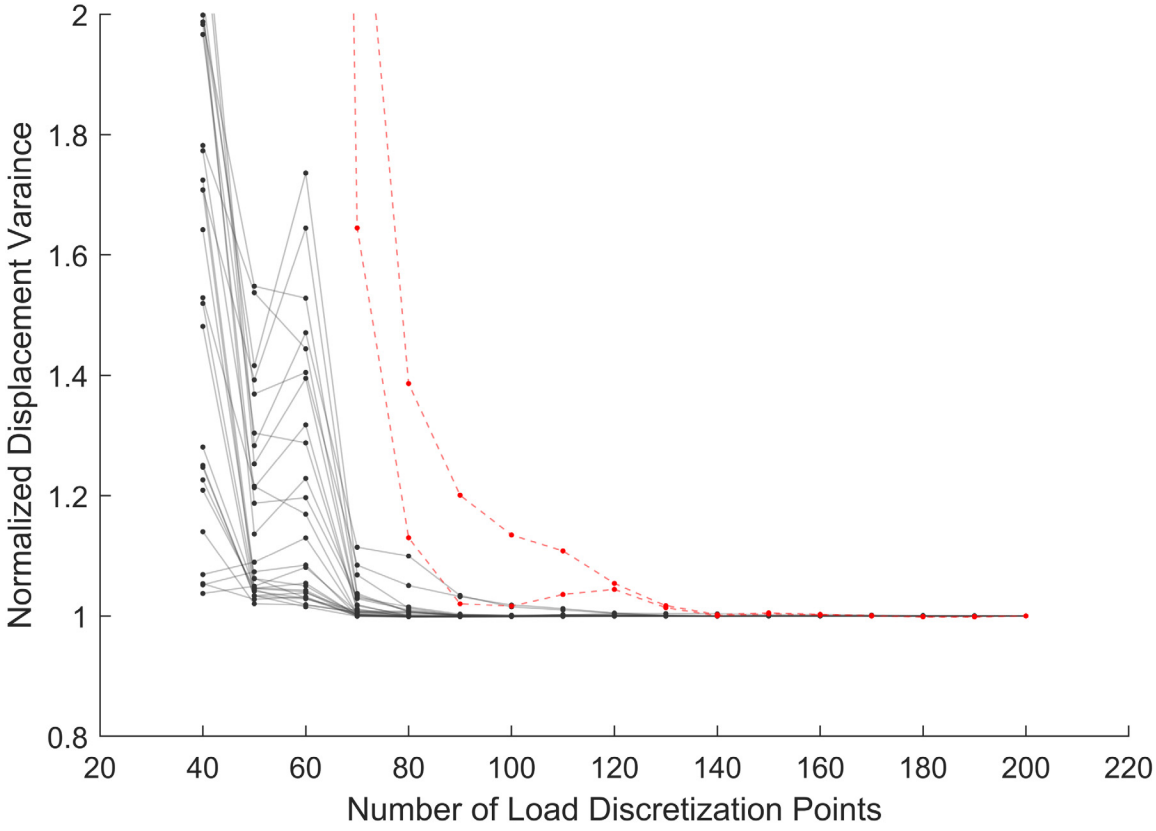

Fig. 9. Convergence of displacement variance at bottom chord nodes with increasing number of load discretization points. The low magnitude responses at interior support locations are highlighted as dashed lines.

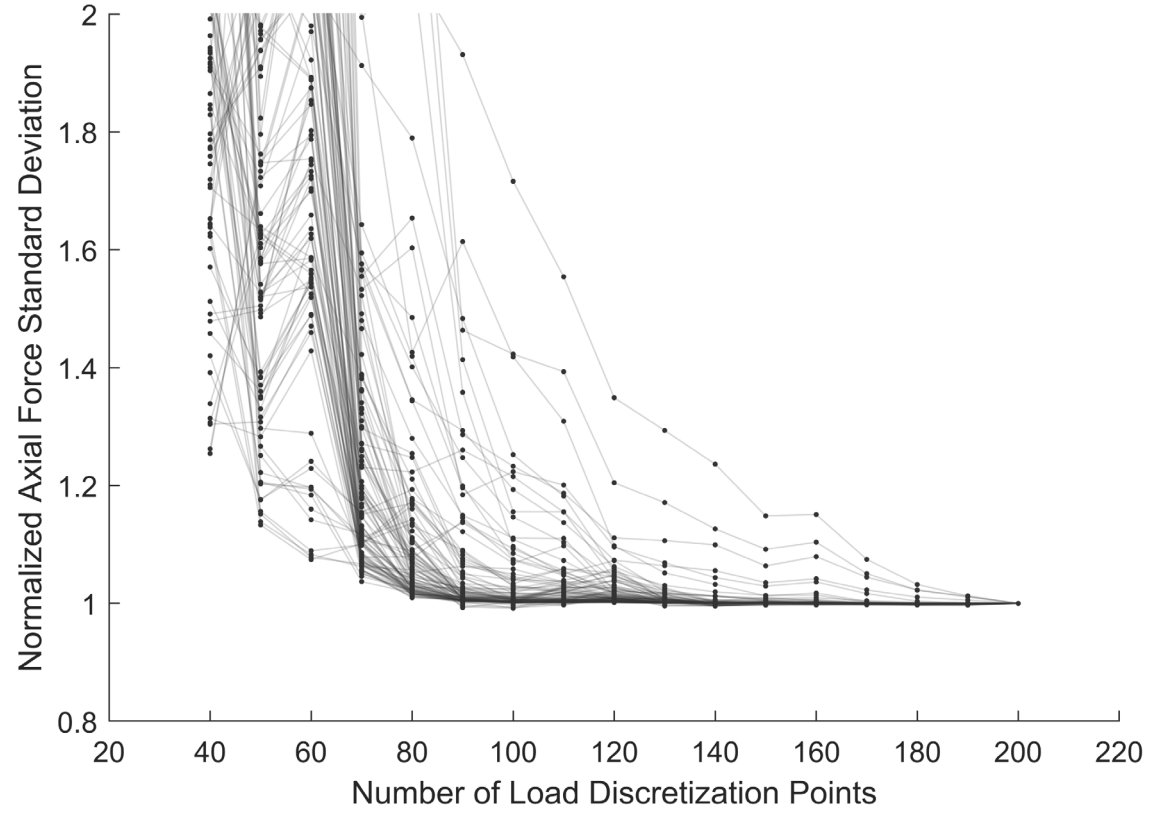

Fig. 10. Convergence of axial force standard deviation with increasing number of load discretization points (excluding zero force members).

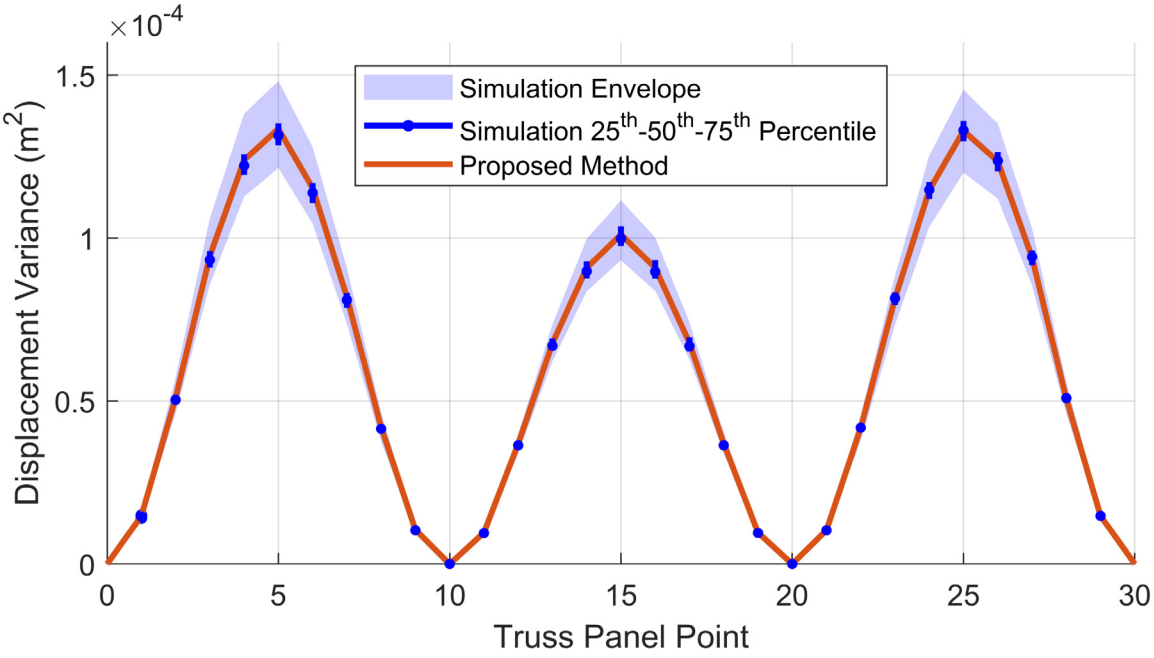

Fig. 11. Comparison of displacement variance between methods at truss bottom chord panel points.

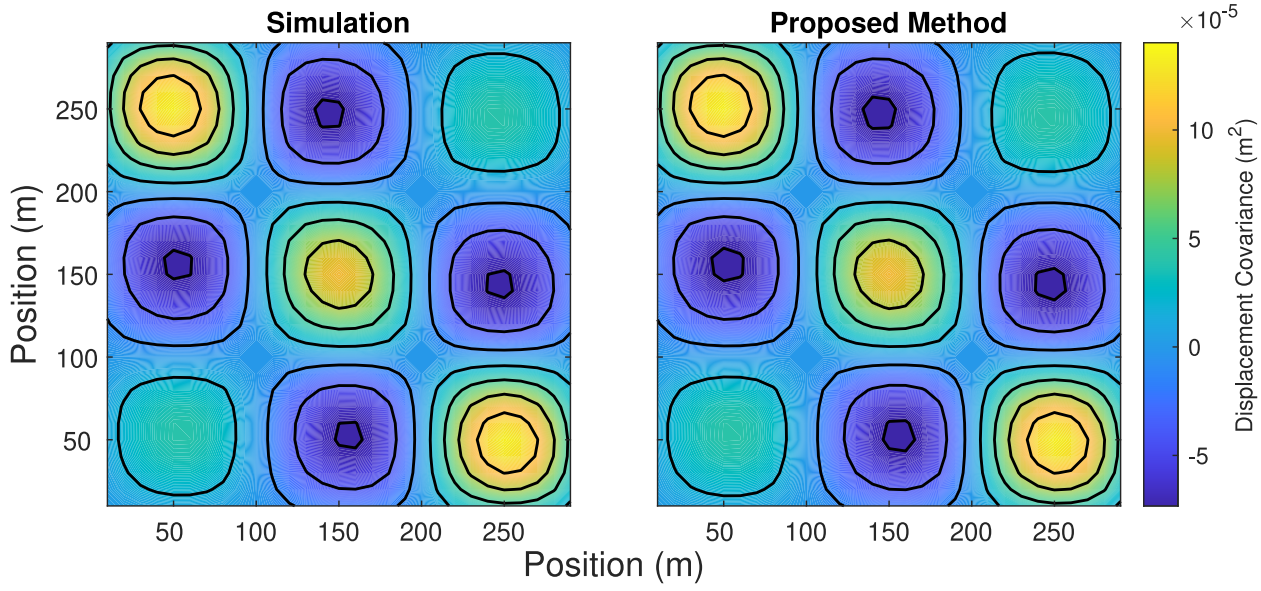

Fig. 12. Comparison of displacement covariance matrix between methods.

approximately 35 min when the loading system had not undergone balanced reduction, and only a few seconds using the reduced loading system. As a comparison, computing 1000 Monte Carlo time domain simulations took approximately 5 min on the same computer, with an Intel Xeon E3- 1285 v6 @4.10 GHz processor and 32 Gb of RAM.

The approach derived here for computing a state space filtered white noise representation of the discrete stochastic moving load process has distinct advantages over the existing methods. Primarily, that it is independent of the structure and enables solving for the response variances quickly using the Lyapunov equation. As a result, this approach lends itself to easily evaluating design alternatives, parametric studies or even structural optimization procedures, where the structural system varies but the loading system remains constant.

Declaration of competing interest

The authors declare that they have no known competing financial interests or personal relationships that could have appeared to influence the work reported in this paper.

Acknowledgments

This work made use of the Illinois Campus Cluster, a computing resource that is operated by the Illinois Campus Cluster Program (ICCP) in conjunction with the National Center for Supercomputing Applications (NCSA) and which is supported by funds from the University of Illinois at Urbana-Champaign, United States.

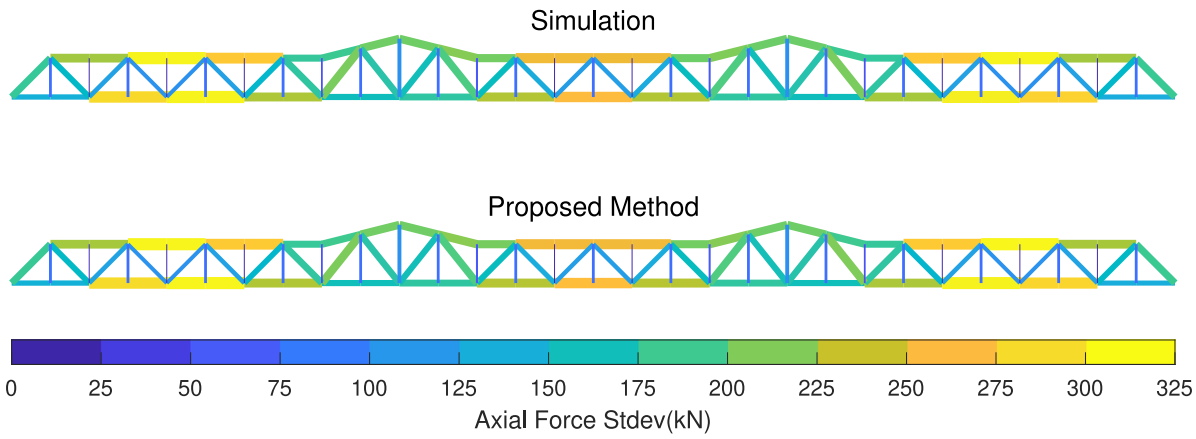

Fig. 13. Comparison of axial force standard deviation between methods.

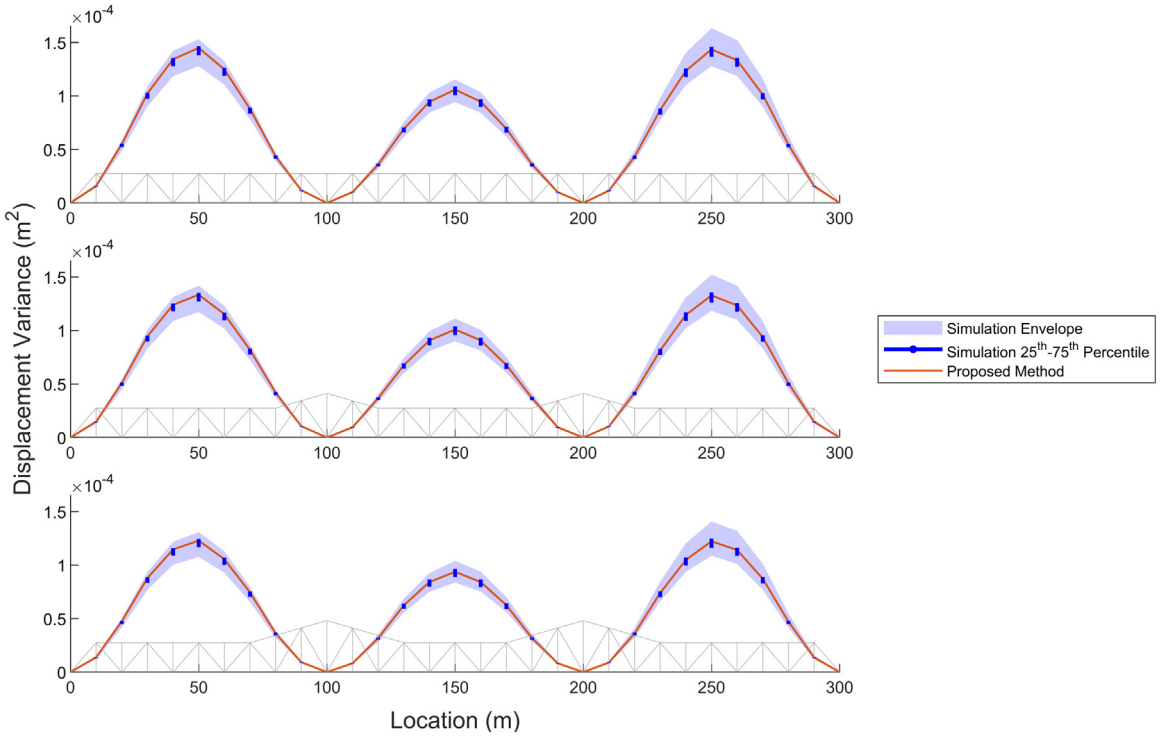

Fig. 14. Displacement variance of bottom chord nodes for alternate truss configurations; top: constant depth truss; middle: baseline truss shown in Fig. 8; bottom: increased depth over interior supports.

Appendix A. Stochastic moving load model with discrete loads

If the moving loads in Eq. (2) were considered as impulse loads rather than distributed, then a similar derivation could be performed. In this case the loads are defined as

$$f_i(x,t) = A_i \delta\left(x - v\left(t - t_i\right)\right) \tag{67}$$

where δ is the Dirac delta.

A function of a random variable, $y = g(x)$ is itself a random variable as long as $g : \mathbb{R} \to \mathbb{R}$. [38,39]. Therefore Eq. (67) does not meet this requirement, because in some sense, the Dirac delta has an infinite value at $\delta(0)$. Nonetheless, the expectation given by $\mathbb{E}[X] = \int_{-\infty}^{\infty} x f(x)\, dx$ is well defined. Proceeding with the derivation in light this ill-defined random variable, the expected value terms of the Dirac delta expressions are

$$\mathbb{E}\left[\delta\left(x - v\left(t - t_i\right)\right)\right] \quad = \frac{1}{vT} \tag{68}$$

and

$$\mathbb{E}\left[\delta\left(x - v\left(t - t_i\right)\right)\delta\left(y - v\left(s - t_i\right)\right)\right] = \frac{1}{v^2 T}\delta\left(\frac{\Delta x}{v} - \tau\right) \tag{69}$$

where $\Delta x = y - x$ and $\tau = s - t$. The resulting auto-covariance function is

$$K(\Delta x, \tau) \quad = \frac{\lambda}{v^2}\delta\left(\frac{\Delta x}{v} - \tau\right)\left(\mu_A^2 + \sigma_A^2\right) \tag{70}$$

The Fourier transform of a Dirac delta is an exponential, i.e., the delay in the time domain is an exponential in the frequency domain

$$S(\Delta x, \omega) = \frac{\lambda\left(\mu_A^2 + \sigma_A^2\right)}{2\pi v^2} e^{-i\omega\frac{\Delta x}{v}} \tag{71}$$

This result agrees with Eq. (36) in the paper.

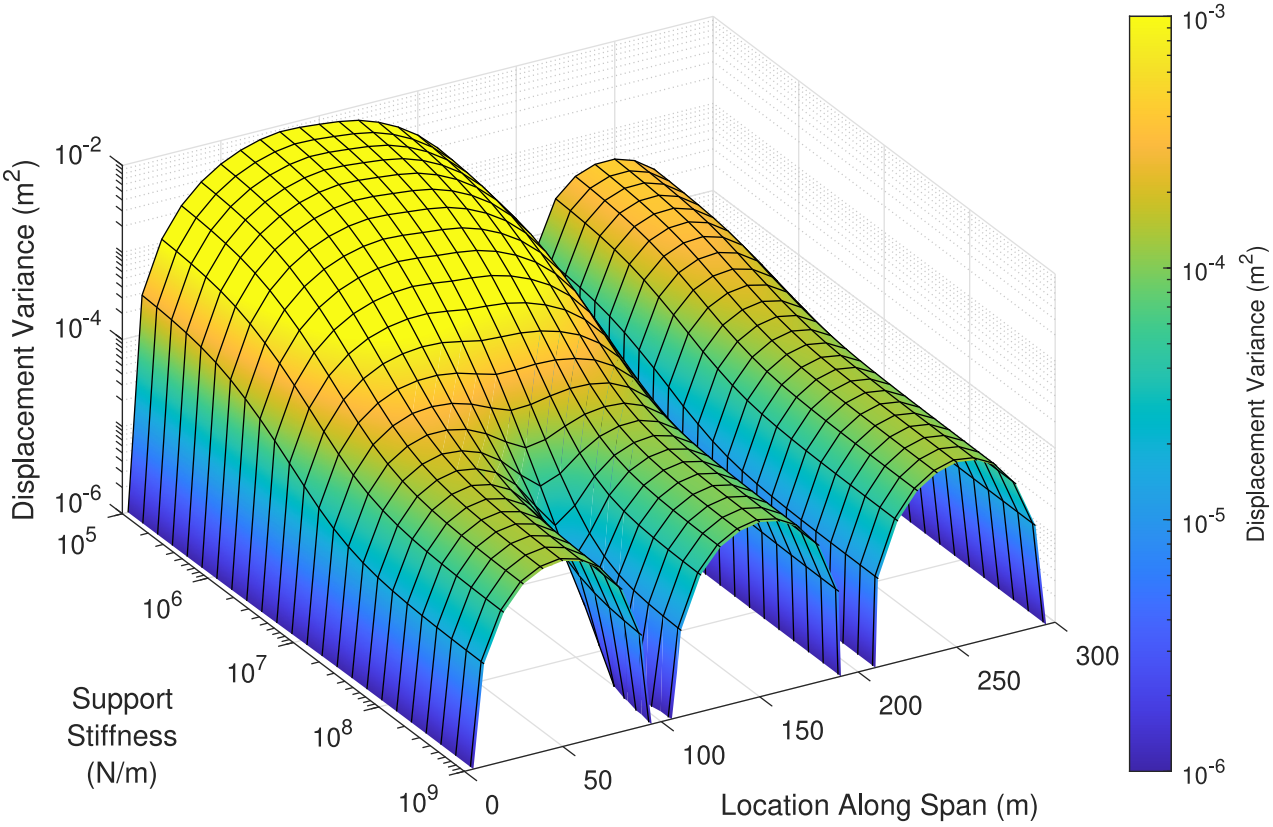

Fig. 15. Displacement variance as a function of support spring stiffness (k_{s1} in Fig. 8).

Appendix B. Modal superposition approach

The classical modal solution of for the moving loads problem typically only employs one mode, resulting in a single-degree-of-freedom problem. This appendix presents the extended classical approach to accommodate structures for which a single mode approximation cannot adequately describe the response.

Assuming proportional damping, the response can be represented as the sum of the modal responses [40] given by

$$u(x,t) = \sum_n q_n(t)\,\phi_n(x) \tag{72}$$

where $\phi_n(x)$ is the nth mode shape, and $q_n(t)$ is the nth modal response. The moving load is a finite duration pulse in time with a shape determined by the mode shape.

$$\gamma_n(t) = \begin{cases} \phi_n(vt) & \text{if } 0 \le t \le \dfrac{L}{v} \\ 0 & \text{if } \dfrac{L}{v} \le t \end{cases} \tag{73}$$

The time domain response of the system to this impulse can be solved using Duhamel's integral.

$$q_n(t) = \begin{cases} \displaystyle\int_0^t \gamma_n(t)\,h_n(t-\tau)\,d\tau & \text{if } 0 \le t \le \dfrac{L}{v} \\ \displaystyle\int_0^{L/v} \gamma_n(t)\,h_n(t-\tau)\,d\tau & \text{if } \dfrac{L}{v} \le t \end{cases} \tag{74}$$

This response is referred to here as the moving load response function. If the moving load impulses can be considered zero mean (via separation of static mean load from the stochastic component), the process is similar to a shot noise process and the response variance can be computed via Campbell's Theorem [41]. Note that the moving load response function needs to consider the period of time while the load is on the span in addition to the free vibration period afterwards. Applying Campbell's Theorem to Eq. (74) yields

$$\sigma^2_{q_n}(t) = \mathbb{E}\left[q_n^2\right] - \mathbb{E}\left[q_n\right]^2 = \mathbb{E}\left[A^2\right]\lambda \int_0^t q_n(\tau)^2\,d\tau \tag{75}$$

where A is the magnitude of the random loads, λ is the arrival rate and $q_n(t)$ represents the moving load response function for that mode and the subscript q_n indicates this covariance is of the modal coordinate, q for mode n.

In early work regarding the response of linear single degree of freedom systems to shot noise, Roberts [42] showed that as the arrival rate increases, the response approaches a normal distribution per the central limit theorem, even for non-normally distributed load magnitudes. For any value of λ, the kth semi-invariant is computed as

$$\eta_k = \mathbb{E}\left[A^k\right]\lambda \int_0^\infty q_n^k(\tau)\,d\tau \tag{76}$$

and the first 5 centered moments μ_k are

$$\begin{aligned} \mu_1 &= \eta_1 \\ \mu_2 &= \eta_2 \\ \mu_3 &= \eta_3 \\ \mu_4 &= \eta_4 + 3\mu_2^2 \\ \mu_5 &= \eta_5 + 10\mu_2\mu_3 \end{aligned} \tag{77}$$

With these equations, the deviation of responses from normally distributed can be assessed.

If the modal frequencies are well separated, the total response variance can then be computed as the sum of modal variances. If the modal frequencies are close to one another, the cross terms in the covariance matrix cannot be neglected. In this case, the full covariance

matrix is computed using an expanded Campbell's Theorem [43–45], as

$$\mathbf{\Gamma_q}(t) = \mathbb{E}\left[\left(q_n - \mu_{q_n}\right)\left(q_m - \mu_{q_m}\right)\right] = \mathbb{E}\left[A^2\right]\lambda \int_0^t q_n(\tau)\, q_m(\tau)\, d\tau \tag{78}$$

This approach was used by Chen et al. [19] on a stochastic moving load to compute covariance of loading functions. The covariance $\mathbf{\Gamma_q}$ in terms of the generalized coordinate q can then be transformed back to the cartesian domain by

$$\mathbf{\Gamma_{yC}} = (\mathbf{\Phi T})\,\mathbf{\Gamma_q}\,(\mathbf{\Phi T})^{\intercal} \tag{79}$$

Where the matrix of mode shapes $\mathbf{\Phi}$ transforms from the generalized coordinates q to the modal coordinate system and the transformation matrix T consists of a column vector for each mode shapes evaluated at selected spatial coordinates. The first numerical examples in Section 4 show that the covariance computed using the expanded Campbell's Theorem, Γ_{yC} is equivalent to that computed using the frequency domain method, as well as the proposed filtered white noise approach.

References

[1] A.S. Nowak, Calibration of LRFD bridge code, J. Struct. Eng. 121 (1995) 1245–1251, http://dx.doi.org/10.1061/(ASCE)0733-9445(1995)121:8(1245).

[2] C. Minervino, B. Sivakumar, F. Moses, D. Mertz, W. Edberg, New AASHTO guide manual for load and resistance factor rating of highway bridges, J. Bridg. Eng. 9 (2004) 43–54, http://dx.doi.org/10.1061/(ASCE)1084-0702(2004)9:1(43).

[3] B. Sivakumar, F.I.S. Ibrahim, Enhancement of Bridge Live Loads using Weigh-in-Motion Data, Vol. 3, IOS Press, 2007, pp. 193–204, http://dx.doi.org/10.1080/15732480701515386.

[4] C.C. Tung, Random response of highway bridges to vehicle loads, J. Eng. Mech. Div. 93 (1967) 79–94, http://dx.doi.org/10.1061/jmcea3.0000896.

[5] J.K. Knowles, On the dynamic response of a beam to a randomly moving load, J. Appl. Mech. Trans. ASME. 35 (1964) 1–6, http://dx.doi.org/10.1115/1.3601165.

[6] L. Frýba, Vibration of Solids and Structures under Moving Loads, Thomas Telford Publishing, 1999, http://dx.doi.org/10.1680/vosasuml.35393.

[7] J.B. Roberts, The response of linear vibratory systems to random impulses, J. Sound Vib. 2 (1965) 375–390, http://dx.doi.org/10.1016/0022-460X(65)90116-1.

[8] Y.K. Lin, Application of nonstationary shot noise in the study of system response to a class of nonstationary excitations, J. Appl. Mech. Trans. ASME 30 (1963) 555–558, http://dx.doi.org/10.1115/1.3636617.

[9] L. Frýba, Non-stationary response of a beam to a moving random force, J. Sound Vib. 46 (1976) 323–338, http://dx.doi.org/10.1016/0022-460X(76)90857-9.

[10] M. Kurihara, T. Shimogo, Vibration of an elastic beam subjected to discrete moving loads, J. Mech. Des. Trans. ASME 100 (1978) 514–519, http://dx.doi.org/10.1115/1.3453960.

[11] R. Iwankiewicz, P. Sniady, Vibration of a beam under a random stream of moving forces, J. Struct. Mech. 12 (1984) 13–26, http://dx.doi.org/10.1080/03601218408907460.

[12] P. Śniady, Dynamic response of linear structures to a random stream of pulses, J. Sound Vib. 131 (1989) 91–102, http://dx.doi.org/10.1016/0022-460X(89)90825-0.

[13] P. Śniady, Vibration of a beam due to a random stream of moving forces with random velocity, J. Sound Vib. 97 (1984) 23–33, http://dx.doi.org/10.1016/0022-460X(84)90464-4.

[14] S. Sorrentino, Power spectral density response of bridge-like structures loaded by stochastic moving forces, Hindawi Shock Vib. (2019) http://dx.doi.org/10.1155/2019/1790480.

[15] R. Iwankiewicz, S.R.K. Nielsen, Linear dynamical systems under random trains of non-overlapping, arbitrary-shape pulses: generalized approach, Probab. Eng. Mech. 19 (2004) 93–104, http://dx.doi.org/10.1016/J.PROBENGMECH.2003.11.008.

[16] A. Jabłonka, R. Iwankiewicz, Dynamic response of a beam to the train of moving forces driven by an erlang renewal process, Probab. Eng. Mech. 66 (2021) 103155, http://dx.doi.org/10.1016/J.PROBENGMECH.2021.103155.

[17] M. Gładysz, P. Śniady, The spectral analysis of a beam under a random train of moving forces, in: Stud. Geotech. Mech. XXIX, 2007.

[18] S.K. Mishra, S.R. Chaudhuri, S. Chakraborty, G. Frantziskonis, Spectral characterization of the stochastically simulated vehicle queue on bridges, Eng. Comput. 25 (2009) 367–378, http://dx.doi.org/10.1007/s00366-009-0130-9.

[19] Y. Chen, C.-A. Tan, M.Q. Feng, Physics-based traffic excitation models for highway bridges, in: S.-C. Liu (Ed.), Smart Struct. Mater. 2004 Sensors Smart Struct. Technol. Civil, Mech. Aerosp. Syst., SPIE, 2004, p. 377, http://dx.doi.org/10.1117/12.540041.

[20] T.T. Soong, M. Grigoriu, Random vibration of mechanical and structural systems, Random Vib. Mech. Struct. Syst. (1993).

[21] J. Xu, B.F. Spencer, X. Lu, X. Chen, L. Lu, Optimization of structures subject to stochastic dynamic loading, Comput. Civ. Infrastruct. Eng. 32 (2017) 657–673, http://dx.doi.org/10.1111/MICE.12274.

[22] F. Gomez, B.F. Spencer, Topology optimization framework for structures subjected to stationary stochastic dynamic loads, Struct. Multidiscip. Optim. 59 (2019) 813–833, http://dx.doi.org/10.1007/s00158-018-2103-3.

[23] F. Gomez, B.F. Spencer, J. Carrion, Topology optimization of buildings subjected to stochastic base excitation, Eng. Struct. 223 (2020) 111111, http://dx.doi.org/10.1016/J.ENGSTRUCT.2020.111111.

[24] F. Gomez, B.F. Spencer, J. Carrion, Topology optimization of buildings subjected to stochastic wind loads, Probabilistic Eng. Mech. 64 (2021) 103127, http://dx.doi.org/10.1016/j.probengmech.2021.103127.

[25] F. Gomez, G.A. Fermandois, B.F. Spencer, Optimal design of nonlinear energy sinks for mitigation of seismic response on structural systems, Eng. Struct. 232 (2021) 111756, http://dx.doi.org/10.1016/j.engstruct.2020.111756.

[26] J. Xu, G.A. Fermandois, B.F. Spencer, X. Lu, Stochastic optimisation of buckling restrained braced frames under seismic loading, Struct. Infrastruct. Eng. 14 (2018) 1386–1401, http://dx.doi.org/10.1080/15732479.2018.1443144.

[27] O. Ditlevsen, Traffic loads on large bridges modeled as white-noise fields, J. Eng. Mech. 120 (1994) 681–694, http://dx.doi.org/10.1061/(ASCE)0733-9399(1994)120:4(681).

[28] O. Ditlevsen, H.O. Madsen, Stochastic vehicle-queue-load model for large bridges, J. Eng. Mech. 120 (1994) 1829–1847, http://dx.doi.org/10.1061/(ASCE)0733-9399(1994)120:9(1829).

[29] T.T. Soong, Fundamentals of Probability, John Wiley & Sons Ltd, 2004.

[30] J. Li, J. Chen, Stochastic Dynamics of Structures, John Wiley & Sons, Ltd, Chichester, UK, 2009, http://dx.doi.org/10.1002/9780470824269.

[31] J. Lam, Model reduction of delay systems using pade approximants, Int. J. Control. 57 (1993) 377–391, http://dx.doi.org/10.1080/00207179308934394.

[32] R.E. Kim, S. Kang, B.F. Spencer, H. Ozer, I.L. Al-Qadi, Stochastic analysis of energy dissipation of a half-car model on nondeformable rough pavement, J. Transp. Eng. Part B Pavements 143 (2017) 04017016, http://dx.doi.org/10.1061/JPEODX.0000014.

[33] J. Sachs, Padé delay is okay today, 2016, www.embeddedrelated.com, https://www.embeddedrelated.com/showarticle/927.php (accessed November 1, 2021).

[34] R.G. Campos, M.L. Calderón, Approximate closed-form formulas for the zeros of the bessel polynomials, Int. J. Math. Math. Sci. 2012 (2012) http://dx.doi.org/10.1155/2012/873078.

[35] F.A. Grünbaum, Variations on a theme of Heine and Stieltjes: an electrostatic interpretation of the zeros of certain polynomials, J. Comput. Appl. Math. 99 (1998) 189–194, http://dx.doi.org/10.1016/S0377-0427(98)00156-3.

[36] Z.-Q. Qu, Model Order Reduction Techniques, Springer London, 2004, http://dx.doi.org/10.1007/978-1-4471-3827-3.

[37] H.S. Zibdeh, R. Rackwitz, Response moments of an elastic beam subjected to Poissonian moving loads, J. Sound Vib. 188 (1995) 479–495, http://dx.doi.org/10.1006/jsvi.1995.0606.

[38] S.M. Ross, Introduction to probability models: Tenth edition, in: Introd. to Probab. Model., Tenth ed., 2009, pp. 1–784, http://dx.doi.org/10.1016/C2009-0-30640-6.

[39] L.D. Lutes, S. Sarkani, Random Vibrations: Analysis of Structural and Mechanical Systems, Elsevier Inc., 2003, http://dx.doi.org/10.1016/B978-0-7506-7765-3.X5000-2.

[40] R.R. Craig, A.J. Kurdila, Fundamentals of Structural Dynamics, Wiley, 2011.

[41] K. Sobczyk, Stochastic Differential Equations, Springer Netherlands, 1991, http://dx.doi.org/10.1007/978-94-011-3712-6.

[42] J.B. Roberts, On the response of a simple oscillator to random impulses, J. Sound Vib. 4 (1966) 51–61, http://dx.doi.org/10.1016/0022-460X(66)90153-2.

[43] E.N. Rowland, The Theory of the Mean Square Variation of a Function formed by Adding known Functions with Random Phases, and Applications to the Theories of the Shot Effect and of Light, Math. Proc. Cambridge Philos. Soc. Vol. 32, 1936, pp. 580–597, http://dx.doi.org/10.1017/S0305004100019319.

[44] L. Cohen, Generalization of Campbell's theorem to nonstationary noise, in: 2014 22nd Eur. Signal Process. Conf., 2014, pp. 2415–2419.

[45] Y.K. Lin, On random pulse train and its evolutionary spectral representation, Probab. Eng. Mech. 1 (1986) 219–223, http://dx.doi.org/10.1016/0266-8920(86)90015-9.